

Hadronic Vacuum Polarization measurement at Belle II

Yuki Sue

Nagoya University

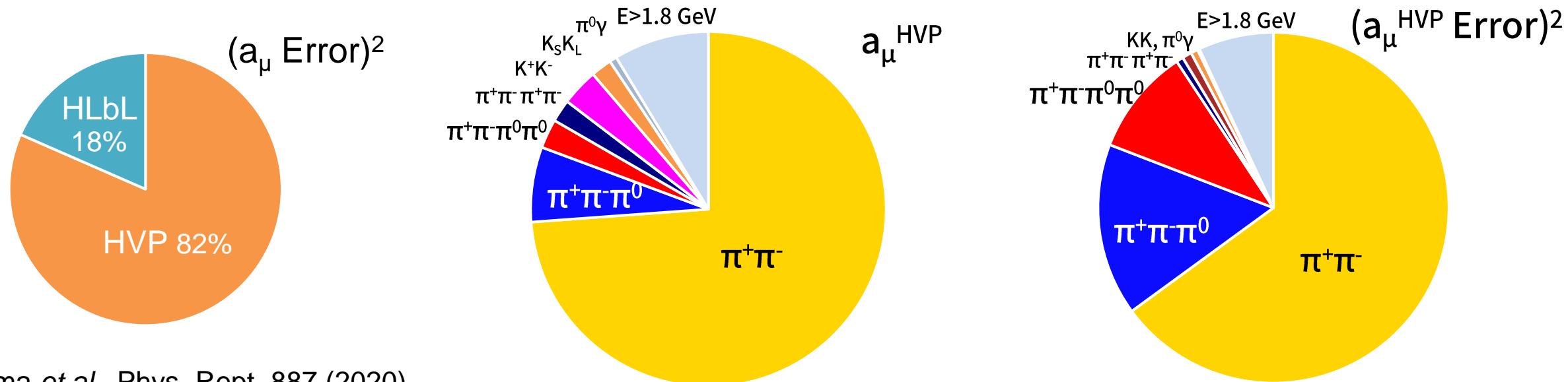
On behalf of the Belle II collaboration

The Muon $g-2$ Theory Initiative Workshop, September 4th-8th, 2023

Muon $g-2$ and Hadronic Vacuum Polarization (HVP)

- HVP contributes to the largest uncertainty in the prediction of muon $g-2$.
- Two approaches for estimating the HVP contribution of SM predictions
 - Dispersion relations (w/ inputs from $ee \rightarrow$ hadrons data)
 - Lattice QCD
- Belle II can provide the cross section for $e^+e^- \rightarrow$ hadrons to improve the theoretical prediction.

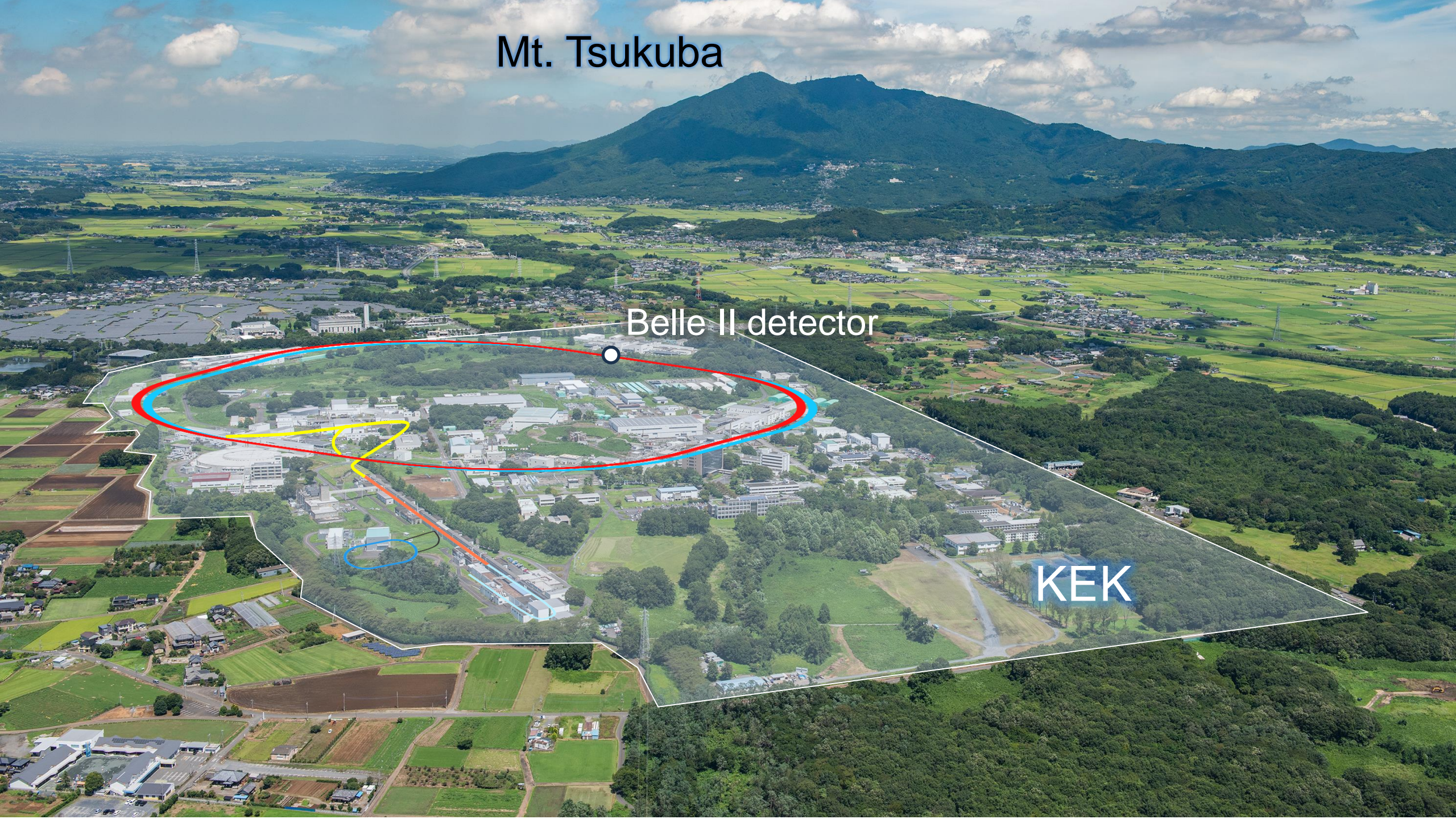
$$a_{\mu}^{\text{SM}} = \frac{g-2}{2} = a_{\mu}^{\text{QED}} + a_{\mu}^{\text{EW}} + a_{\mu}^{\text{Had}}$$



Mt. Tsukuba

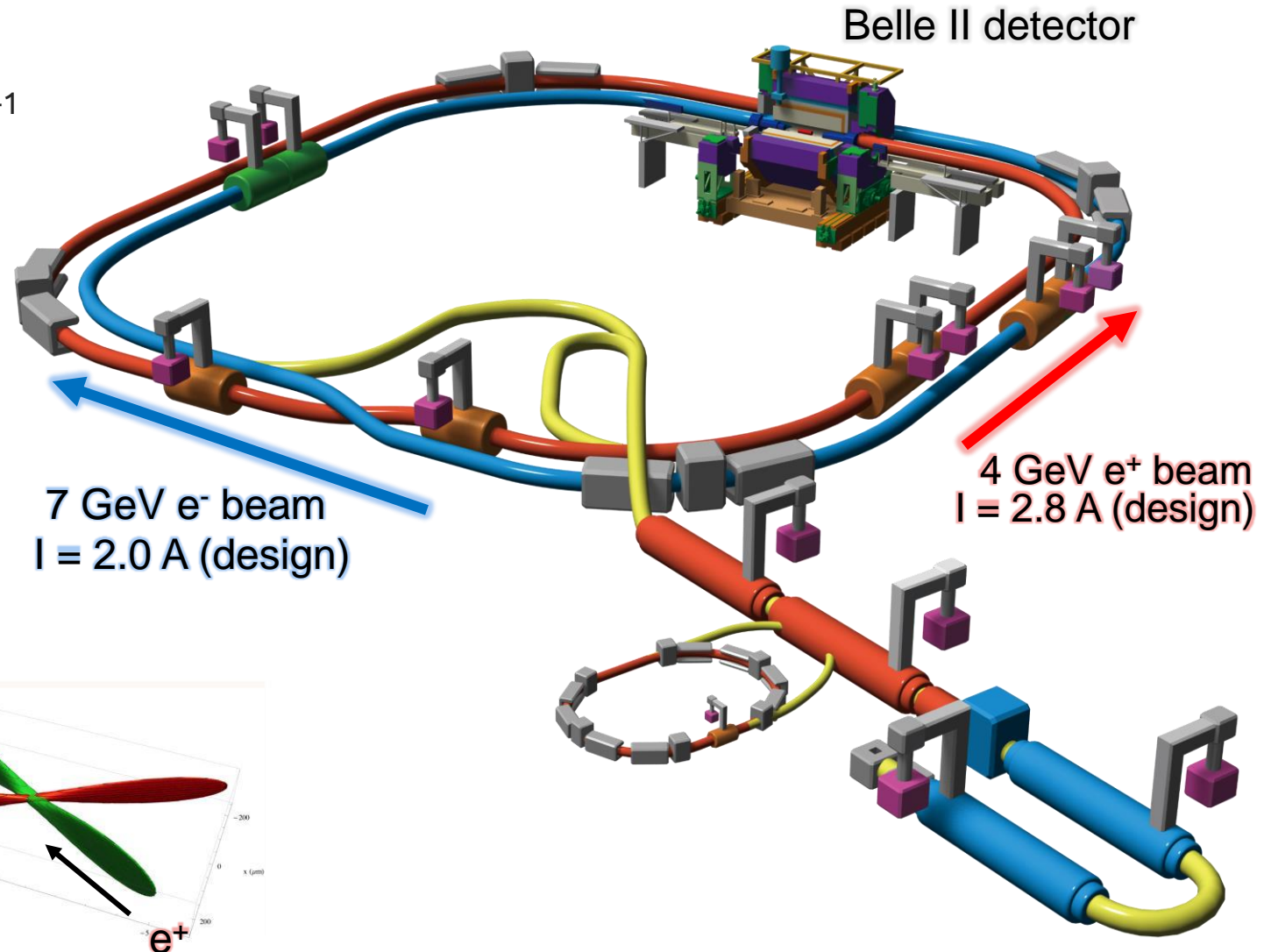
Belle II detector

KEK

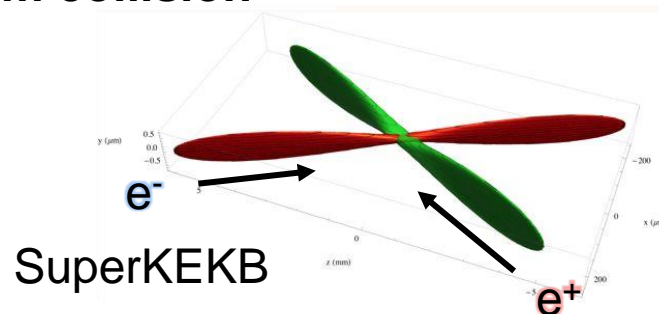
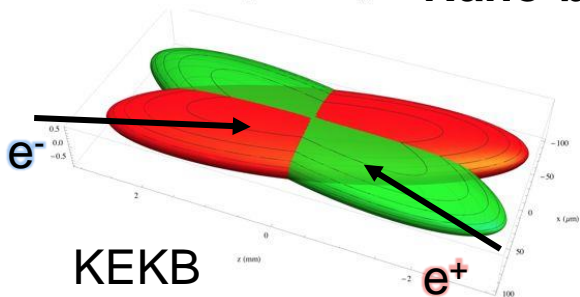


SuperKEKB collider

- Asymmetric e^+e^- collider
 - $\sqrt{s} = M(Y(4S)) = 10.58 \text{ GeV}$
 - Design luminosity : $6 \times 10^{35} \text{ cm}^{-2}\text{s}^{-1}$
- Improvements from KEKB
 - Nano beam scheme
 - Higher beam currents



Nano-beam collision



Belle II detector

Particle Identification

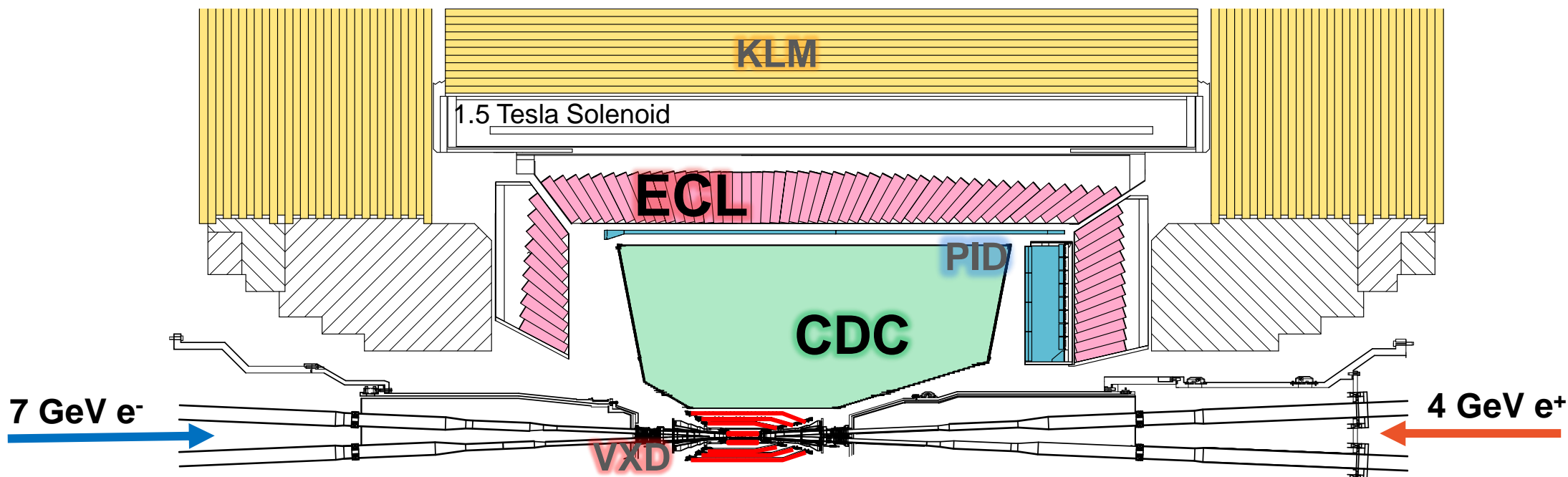
- Aerogel RICH in the forward endcap
- Time-of-Propagation counter in the barrel
- **K/ π ID : K efficiency 90% at 1.8% π fake**

Electromagnetic Calorimeter (ECL)

- CsI(Tl) crystals + Waveform sampling
- **Electron ID eff. 90% at <0.1% fake**
- **Energy resolution 1.6-4%**
- **94% of solid angle coverage**

K-long and Muon Detector (KLM)

- Alternating iron and detector plates
- Scintillator / Resistive Plate Chamber
- **Muon ID efficiency 90% at 2% fake**



Vertex Detector (VXD)

- Inner 2 layers : Pixel
- Outer 4 layer : Double side strip
- $\sigma(\text{Track impact parameter}) \sim 15 \mu\text{m}$

Central Drift Chamber (CDC)

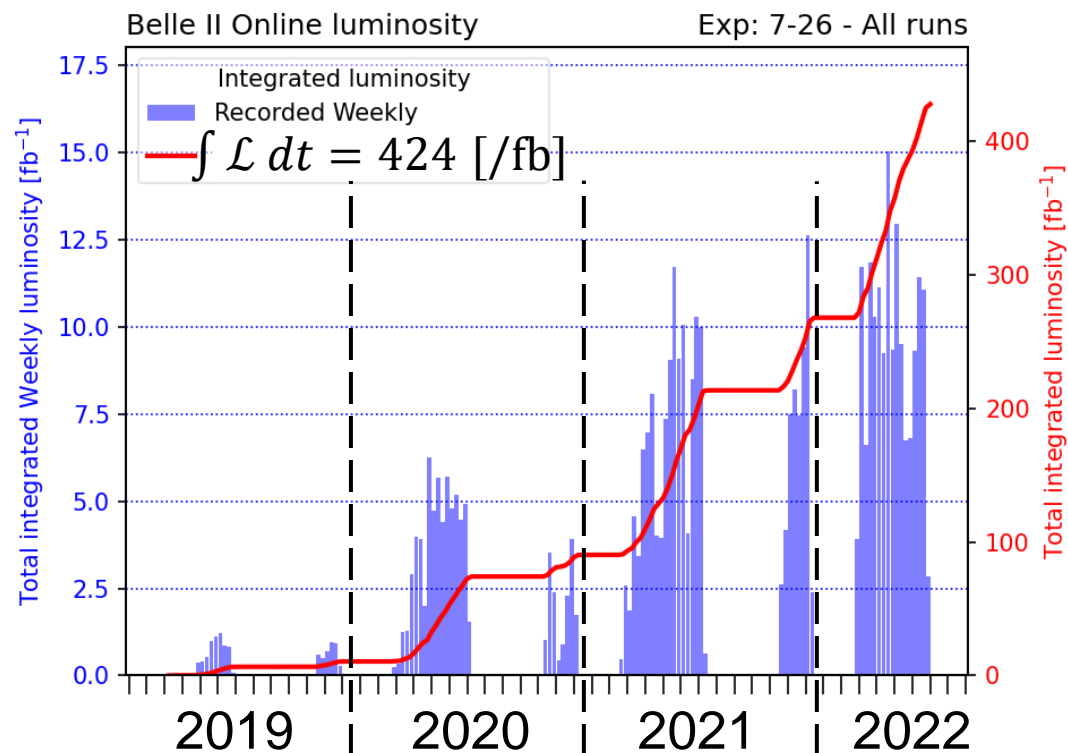
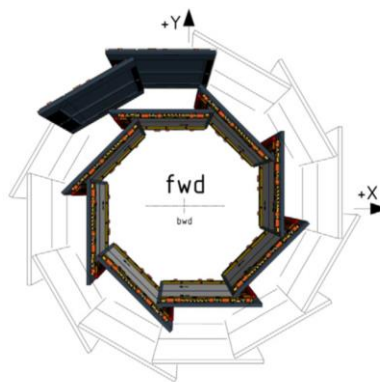
- **91% of solid angle coverage**
- **p_T resolution $\sim 0.4\%/p_T$**
- **dE/dx resolution 5% (low-p PID)**

Trigger and DAQ

- L1 Trigger rate 30 kHz (design)
- **New trigger line for low-multiplicity events**
- Constant improvements of trigger algorithm

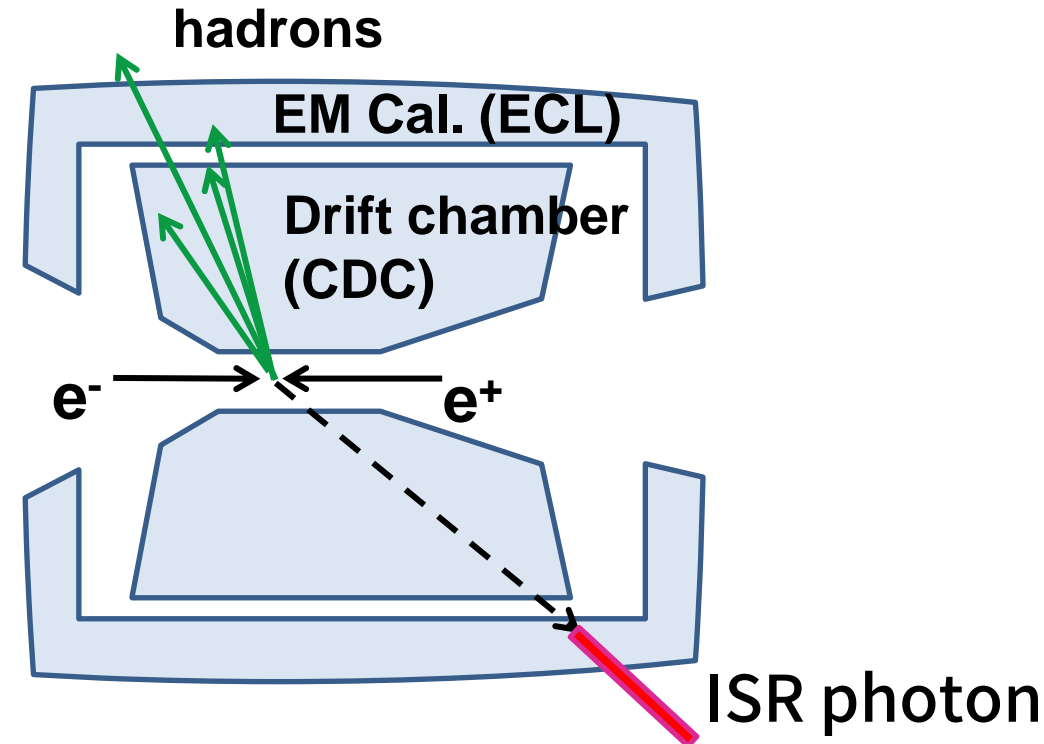
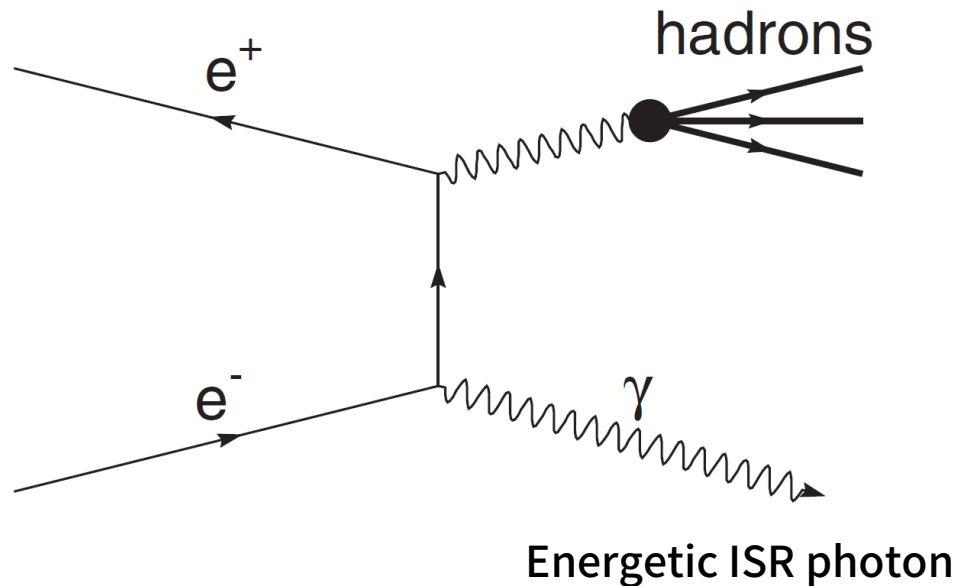
Operation status

- World record instantaneous luminosity : 4.7×10^{34} /cm²/s
 - ~90% data taking efficiency : 1-2 fb⁻¹/day
- Recorded data : 424 /fb
 - 363 fb⁻¹ at $\sqrt{s} = 10.58$ GeV
- Long Shutdown 1 is finishing and new run will start at the end of 2023.
 - SuperKEKB upgrade for higher luminosity etc.
 - Full coverage of pixel detector
 - PMT replacement of the barrel PID detector for lifetime and robustness
 - Data-acquisition system upgrade



Radiative return method for HVP measurements

- Radiative return is also used in BaBar, KLOE, BESIII
 - Other method is direct scan, e.g., Novosibirsk experiments
- Scan the energy of hadronic system at fixed energy using ISR
- Access to the entire hadronic mass range with single dataset
- Around 7% of ISR photons are produced within the detector acceptance.

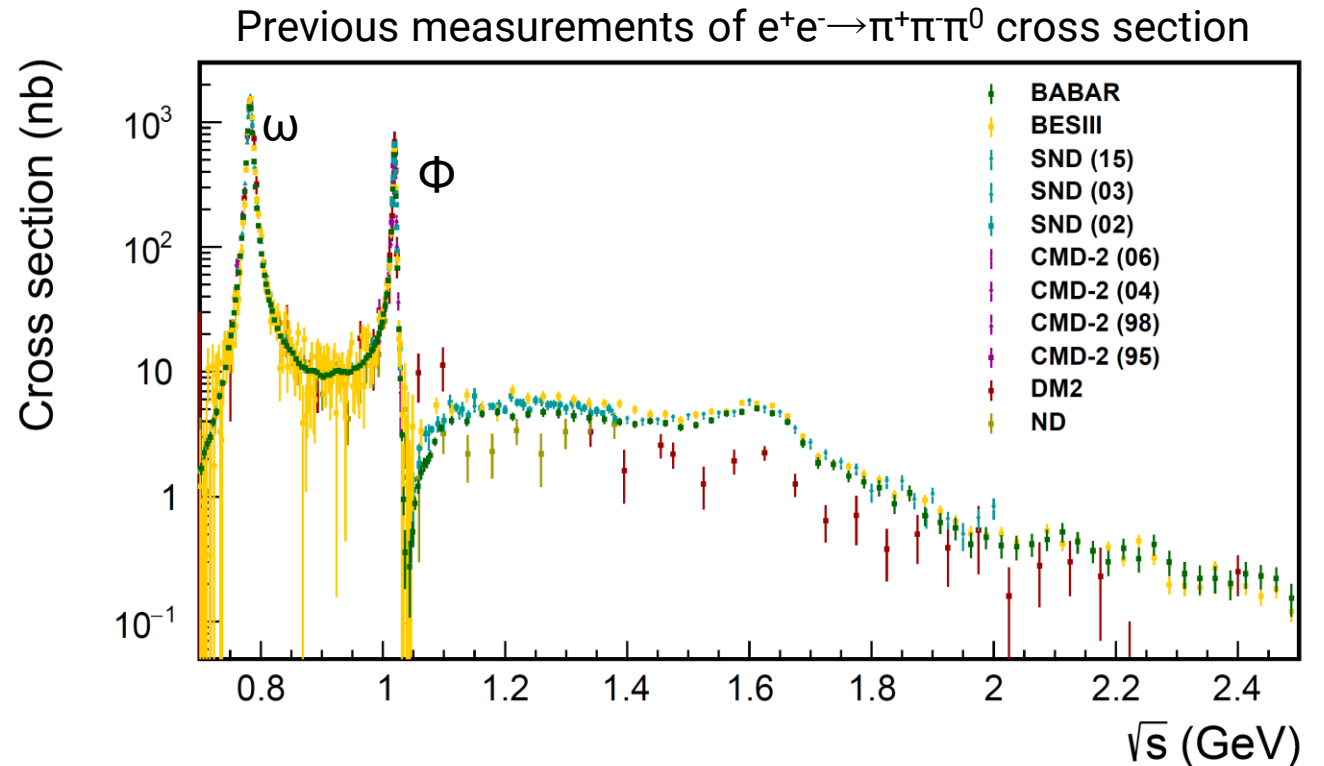


HVP measurements at Belle II

- **New low-multiplicity trigger** lines enable this physics at Belle II
 - Almost 100% efficiency for energetic ISR
 - Two independent triggers : Tracker and Calorimeter
- Two channels are mainly under study
 1. $e^+e^- \rightarrow \pi^+\pi^-$
 - The largest contribution to $a_\mu^{\text{HVP}} \sim 73\%$
 - Target 0.5% precision using 363 fb^{-1} data
 - Try to following BaBar methods as a base line
 2. $e^+e^- \rightarrow \pi^+\pi^-\pi^0$
 - The 2nd largest contribution to $a_\mu^{\text{HVP}} \sim 7\%$
- Today we report the status of $e^+e^- \rightarrow \pi^+\pi^-\pi^0$ analysis to demonstrate the capability of Belle II for the ISR processes

Previous measurements of $e^+e^- \rightarrow \pi^+\pi^-\pi^0$

- Recent measurements
 - Preliminary result from BES III [[arXiv:1912.11208](https://arxiv.org/abs/1912.11208)]
 - BABAR has updated its results with full data [[Phys. Rev. D 104, 112003 \(2021\)](https://arxiv.org/abs/2103.11203)]
- As for the $e^+e^- \rightarrow \pi^+\pi^-\pi^0$ contribution $a_\mu(3\pi)$, the uncertainty of $a_\mu(3\pi)$ is 2-3% for combination and 1.3% for BABAR alone
 - The difference in the cross section between the experiments below 1.1 GeV produces the error.



[Eur. Phys. J. C 80, 241 \(2020\)](https://arxiv.org/abs/2005.04822)

[Phys. Rev. D 101, 014029 \(2020\)](https://arxiv.org/abs/2005.04822)

[J. High Energy Phys. 08 137 \(2019\)](https://arxiv.org/abs/1905.04822)

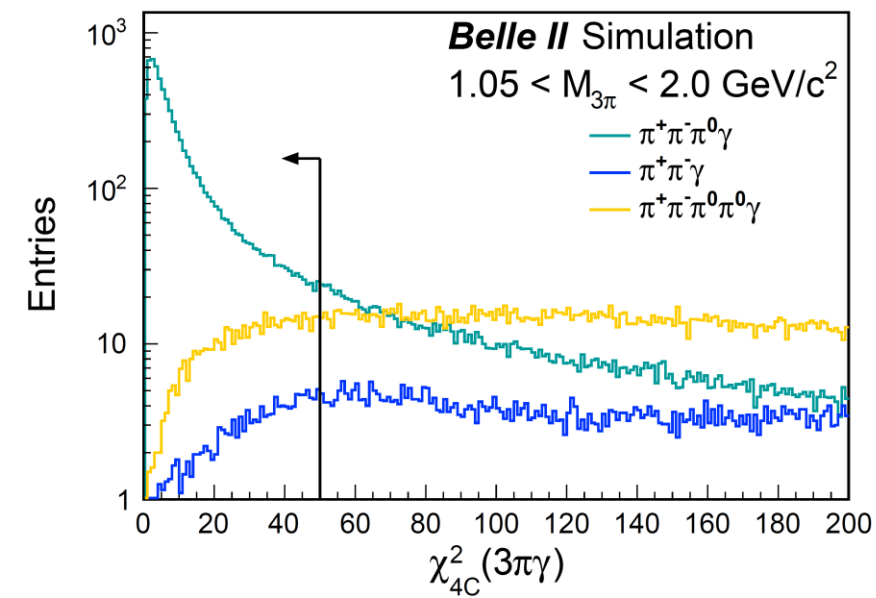
$e^+e^- \rightarrow \pi^+\pi^-\pi^0$ Analysis overview

- Target precision : $\delta a_\mu(3\pi) \sim 2\%$
- $\pi^+\pi^-\pi^0$ Mass range : 0.6-3.5 GeV
- Dataset : 2019-2021 Summer 190 fb⁻¹
- Key items
 - Trigger
 - Background reduction and estimation
 - Efficiency corrections
 - Unfolding
- Blind analysis
 - Study of analytical methods using MC and validation using 10% data
 - Final confirmation under way using full data without correction factors

$e^+e^- \rightarrow \pi^+\pi^-\pi^0$: Event selection

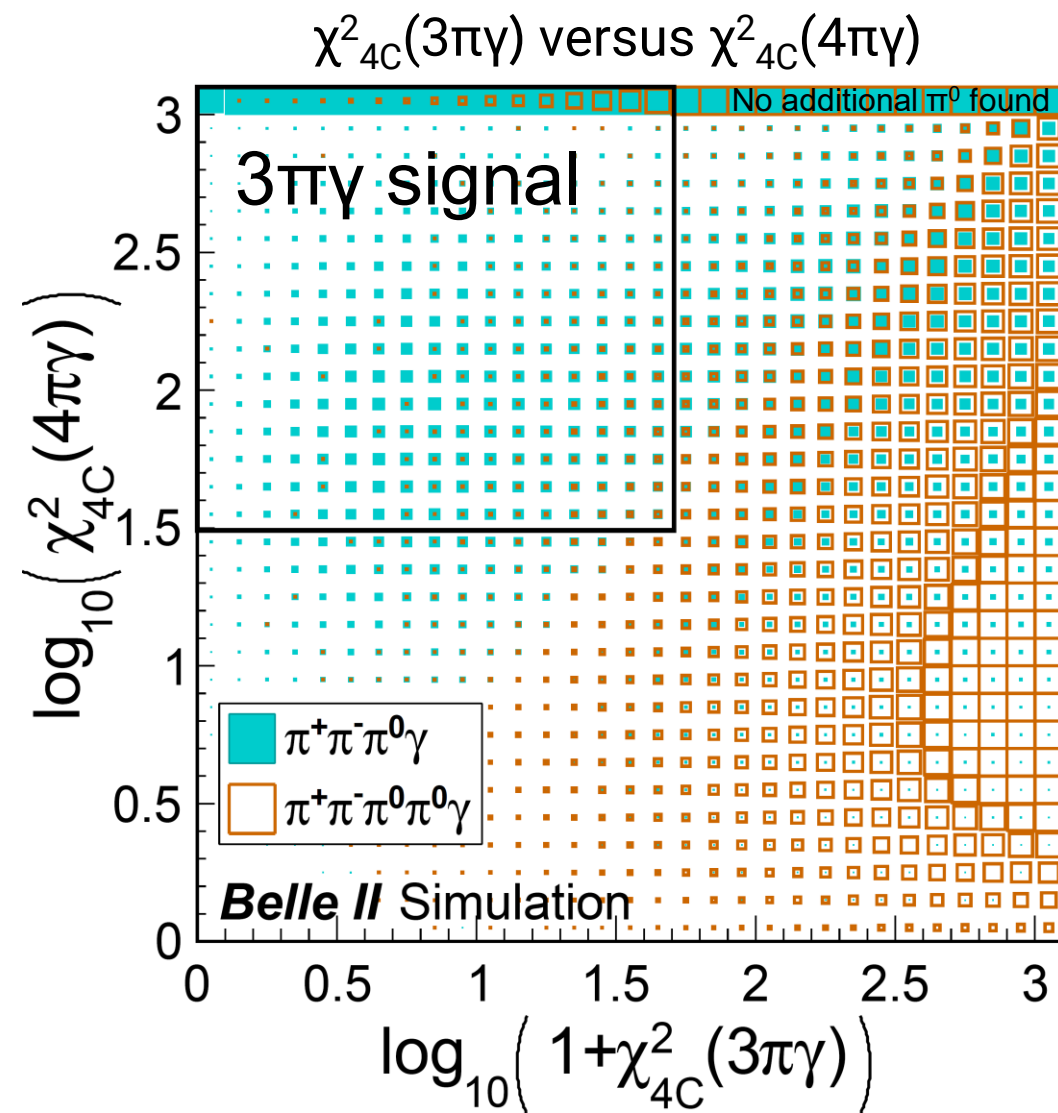
- Two tracks + three photons : $e^+e^- \rightarrow \pi^+\pi^-\pi^0\gamma_{\text{ISR}} \rightarrow \pi^+\pi^-\gamma\gamma\gamma_{\text{ISR}}$
 - Tracks : $dr < 0.5$ cm and $|dz| < 2$ cm and $p_T > 0.2$ GeV/c
 - Photons : $E > 100$ MeV + at least one photon must be energetic ISR ($E^{\text{CMS}} > 2$ GeV in barrel ECL)
- π^0 reconstruction
 - Invariant mass of two photons within 0.123-0.147 GeV/c²
- Select events using four-momentum kinematic fit (4C-Kfit) χ^2
 - $\chi^2_{4C}(3\pi\gamma) < 50$ is used for the cross section measurement
- Cuts to reduce remaining backgrounds
 - A) Background not containing real π^0 : $e^+e^- \rightarrow e^+e^-\gamma, \pi^+\pi^-\gamma, \mu^+\mu^-\gamma$
 - B) Charged kaon : $e^+e^- \rightarrow K^+K^-\pi^0\gamma$
 - C) $e^+e^- \rightarrow \pi^+\pi^-\pi^0\pi^0\gamma$
 - D) Background not containing real ISR : Non-ISR $q\bar{q}$ and $\tau^+\tau^-$

4C-Kfit χ^2 distribution
in $M(3\pi) > 1.05$ GeV



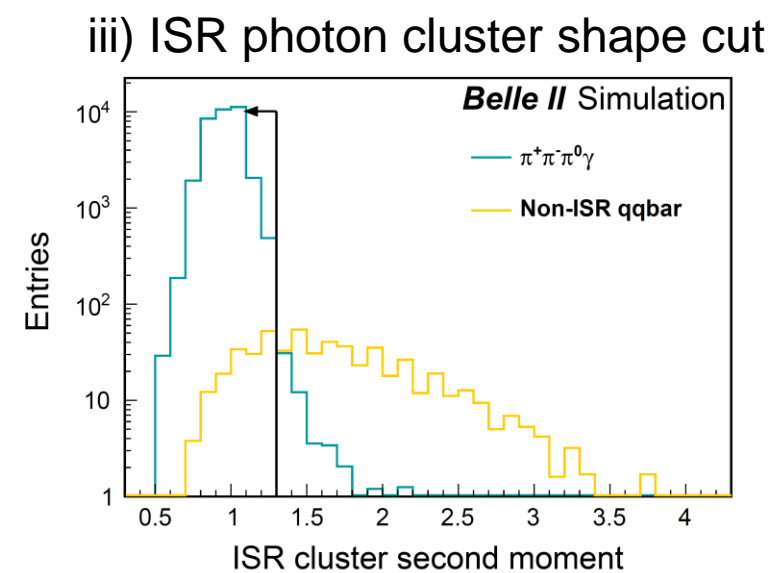
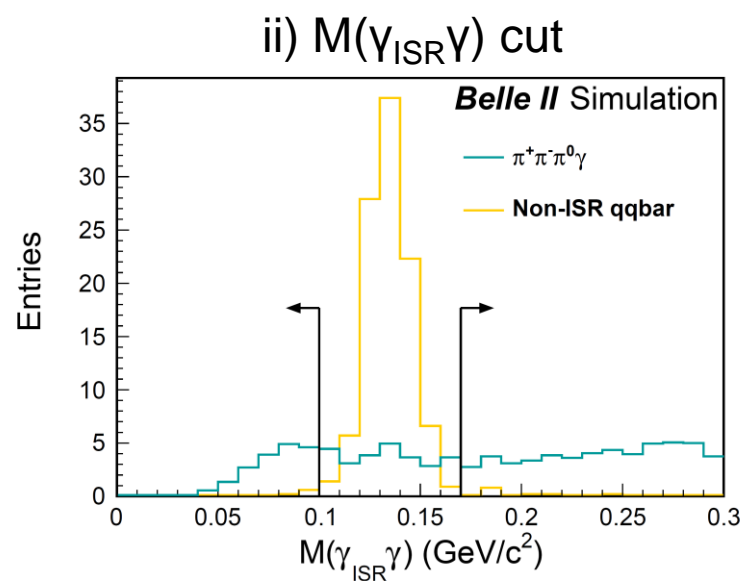
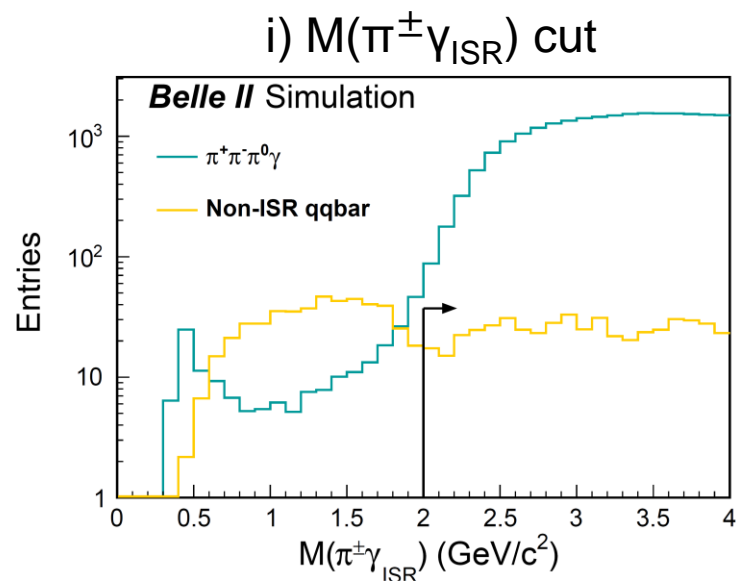
Background reduction cuts (1)

- A) Background not containing real π^0 : $e^+e^- \rightarrow e^+e^-\gamma, \pi^+\pi^-\gamma, \mu^+\mu^-\gamma$
- Pion/Electron ID : $L(\pi/e) > 0.1$
 - $M^2_{\text{recoil}}(\pi^+\pi^-) > 4 \text{ GeV}^2/c^4$
- B) Charged kaon : $e^+e^- \rightarrow K^+K^-\pi^0\gamma$
- Pion/Kaon ID : $L(\pi/K) > 0.1$
- C) $e^+e^- \rightarrow \pi^+\pi^-\pi^0\pi^0\gamma$
- Reconstruct $\pi^+\pi^-\pi^0\pi^0\gamma$ (with additional π^0)
 - 4C kinematic fit under $\pi^+\pi^-\pi^0\pi^0\gamma$ hypothesis and $\chi^2_{4C}(4\pi\gamma) > 30$



Background reduction cuts (2)

- D) Background not containing real ISR : Non-ISR qqbar (dominated by $\pi^+\pi^-\pi^0\pi^0$) and $\tau^+\tau^-$
- $M(\pi^\pm\gamma_{\text{ISR}}) > 2 \text{ GeV}/c^2$ to reduce high momentum $\rho^\pm \rightarrow \pi^+\pi^0$
 - $M(\gamma_{\text{ISR}}\gamma)$ cut to reduce ISR as which a daughter photon of π^0 is reconstructed
 - Cluster shape cut to reduce ISR as which both photon clusters of π^0 decay are merged.



In total,

$M(3\pi) < 1.05 \text{ GeV}/c^2$: the background fraction is reduced from 8.9% to 2.2% with 9% signal loss.

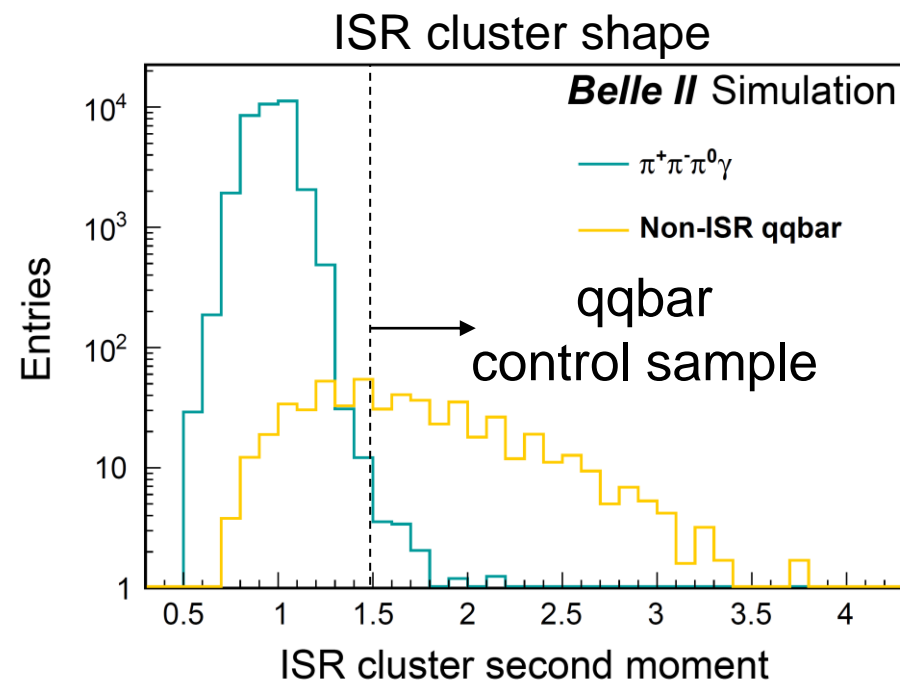
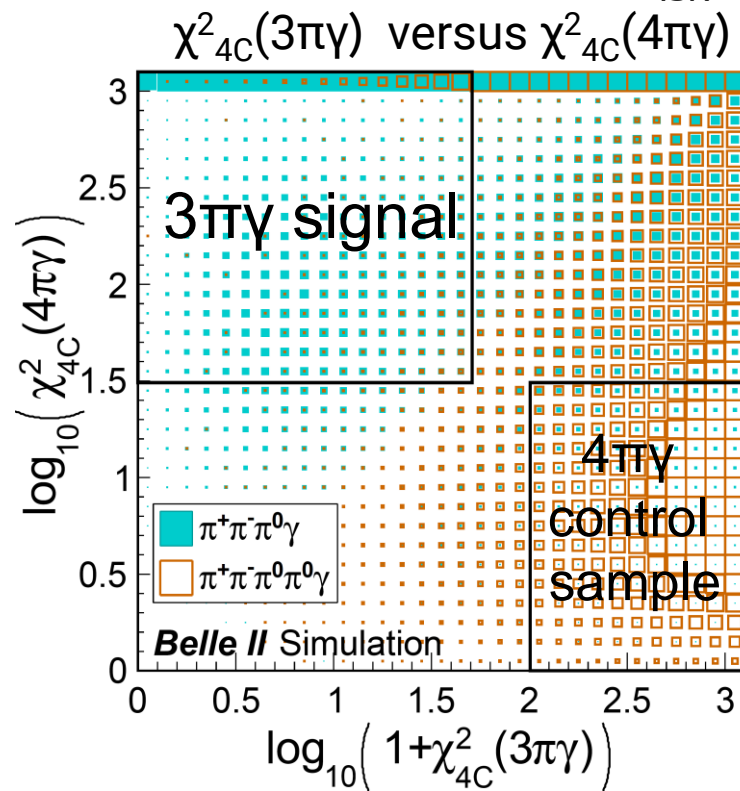
$M(3\pi) > 1.05 \text{ GeV}/c^2$: the background events are reduced 78% with 11% signal loss.

Background estimation

Estimate by determining a mass-dependent data-MC scale factor using a control sample (CS)

$$N_{\text{Signal}}^{\text{data}} = N_{\text{Signal}}^{\text{MC}} \cdot \frac{N_{\text{Control}}^{\text{data}}}{N_{\text{Control}}^{\text{MC}}}$$

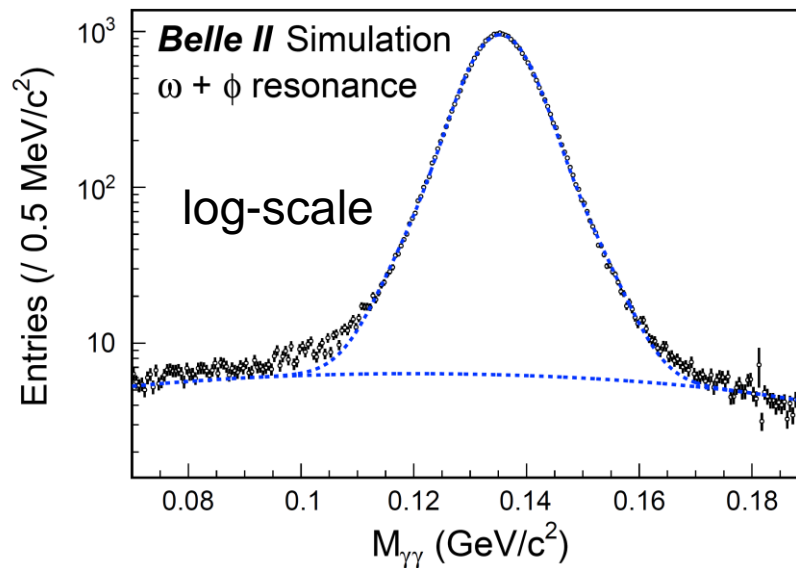
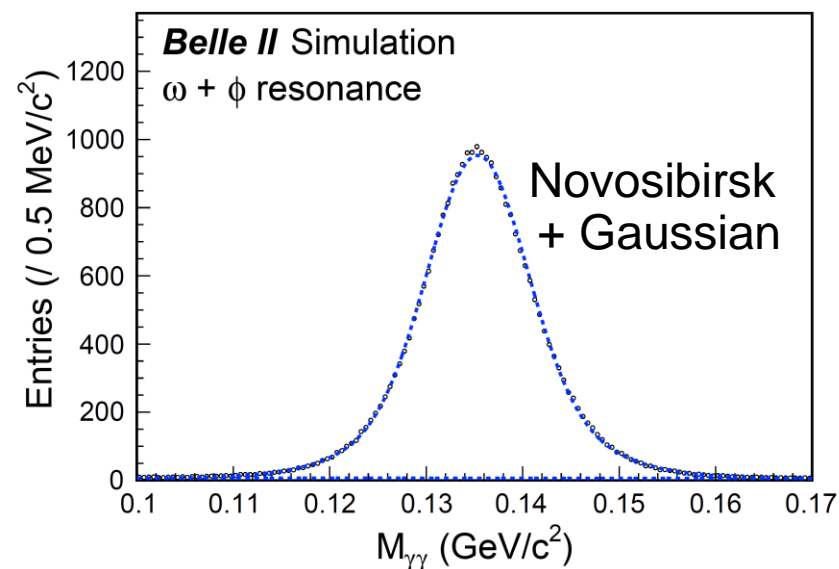
- $e^+e^- \rightarrow K^+K^-\pi^0\gamma$: Invert π/K ID : $L(\pi/K) > 0.1 \Rightarrow L(\pi/K) < 0.1$
- $e^+e^- \rightarrow \pi^+\pi^-\pi^0\pi^0\gamma$: Reconstruct $\pi^+\pi^-\pi^0\pi^0\gamma$ and select $\chi^2(4\pi\gamma) < 30$
- Non-ISR $q\bar{q}$: $0.10 < M(\gamma_{\text{ISR}}\gamma) < 0.17$ GeV / large cluster second moment



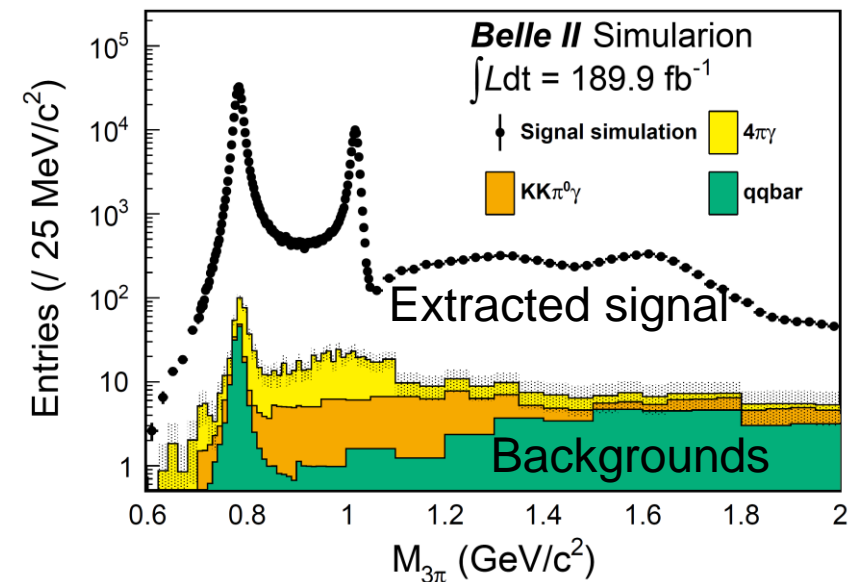
Signals after event selection

- Signal extraction by $M(\gamma\gamma)$ fit to each $M(3\pi)$ bin
 - Fit and integral over 0.123-0.147 GeV/c^2
- Estimated background is subtracted from the spectrum

$\gamma\gamma$ invariant mass fitting

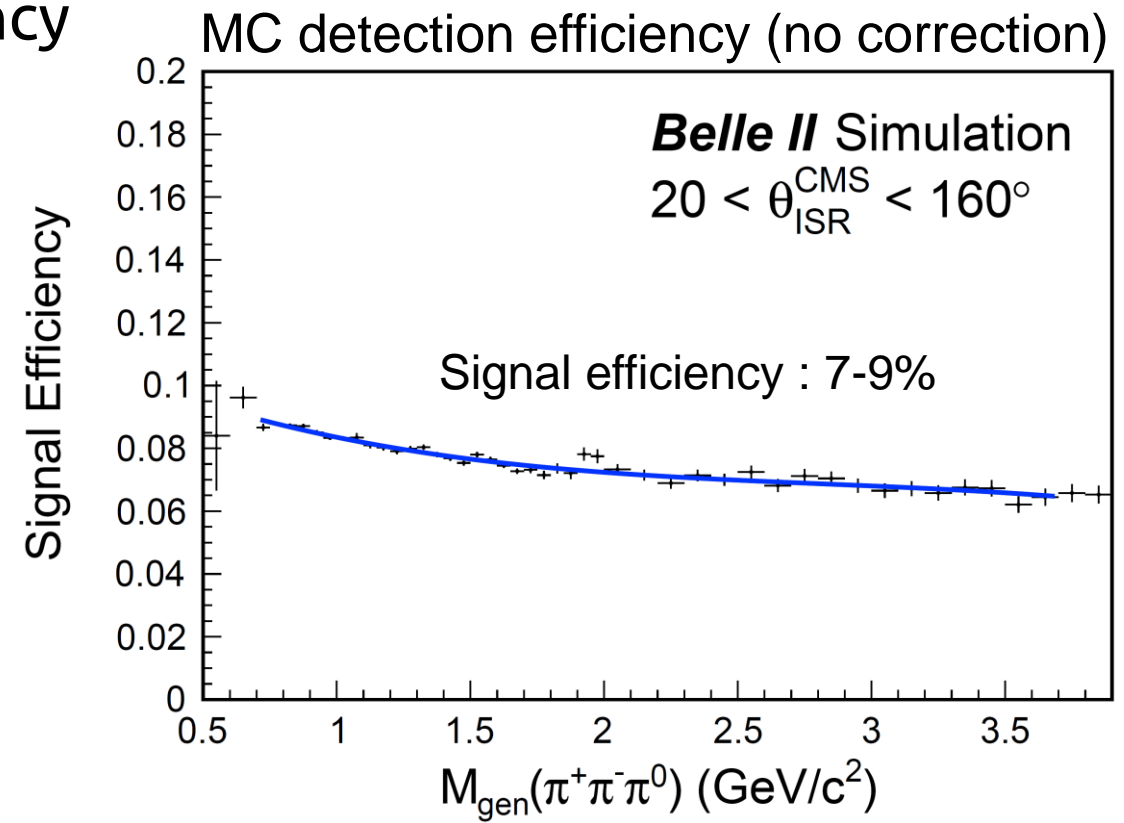


Extracted spectrum and background



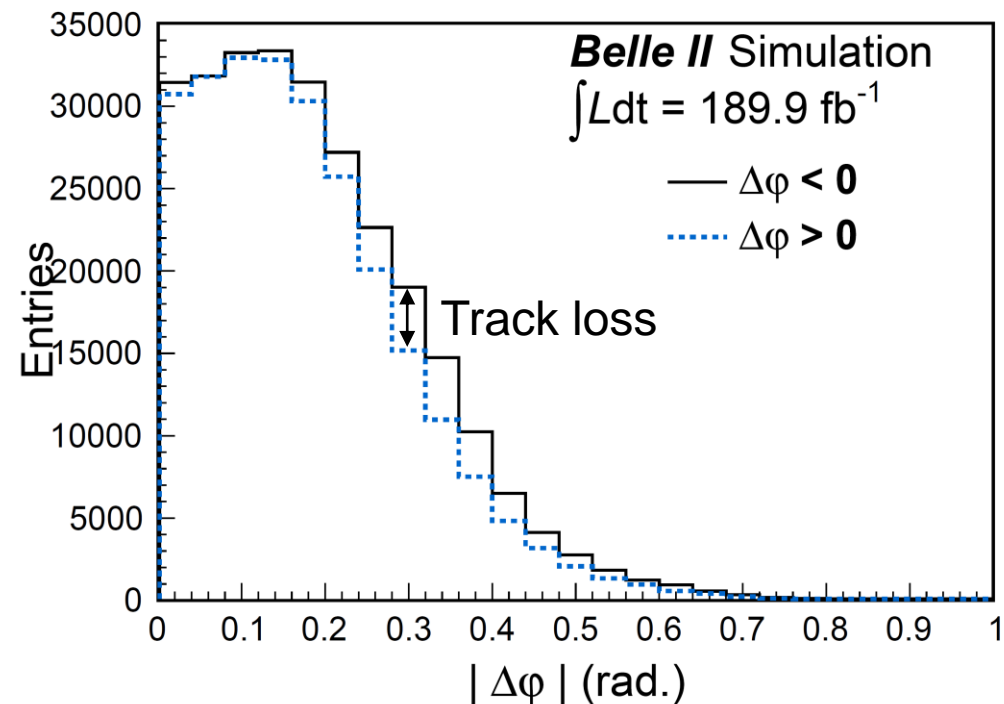
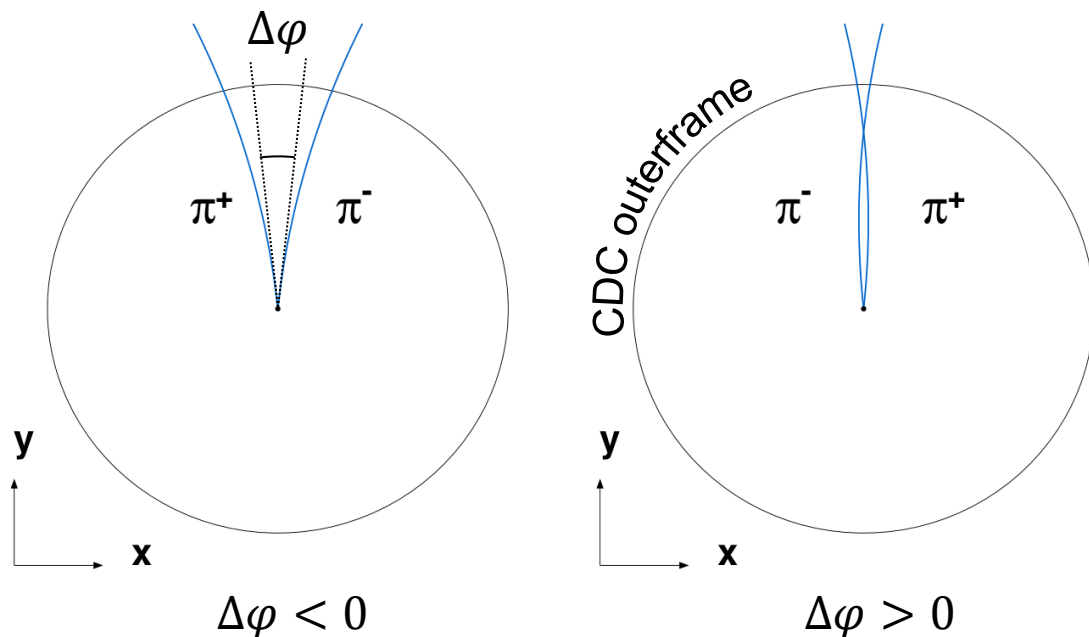
Detection efficiency and Data-MC correction

- Detection efficiency is estimated using MC of the x20 larger statistics.
- Possible differences between data and MC must be corrected.
- Estimate data-MC corrections dedicated to this analysis.
 - Trigger efficiency
 - High energy photon detection efficiency
 - Tracking efficiency
 - π^0 efficiency
 - χ^2 distribution
 - Background reduction cut efficiency



Tracking efficiency

- Tracking efficiency is confirmed by tag-and-probe method using τ pairs.
- Track loss due to crossing on the drift chamber is confirmed.
 - Evaluate using the $e^+e^- \rightarrow \pi^+\pi^-\pi^0\gamma$ process at the ω resonance.
- Define $\Delta\varphi := \varphi(\pi^+) - \varphi(\pi^-)$
- The expected inefficiency due to track loss is $f = \frac{N(\Delta\varphi < 0) - N(\Delta\varphi > 0)}{2N(\Delta\varphi < 0)}$
 - The track loss in MC is 4%.
- In total, the systematic uncertainty of tracking is 0.8%.



π^0 efficiency correction

π^0 detection efficiency is 50-60%.

Evaluate efficiency using the $e^+e^- \rightarrow \pi^+\pi^-\pi^0\gamma$ events of ω resonance.

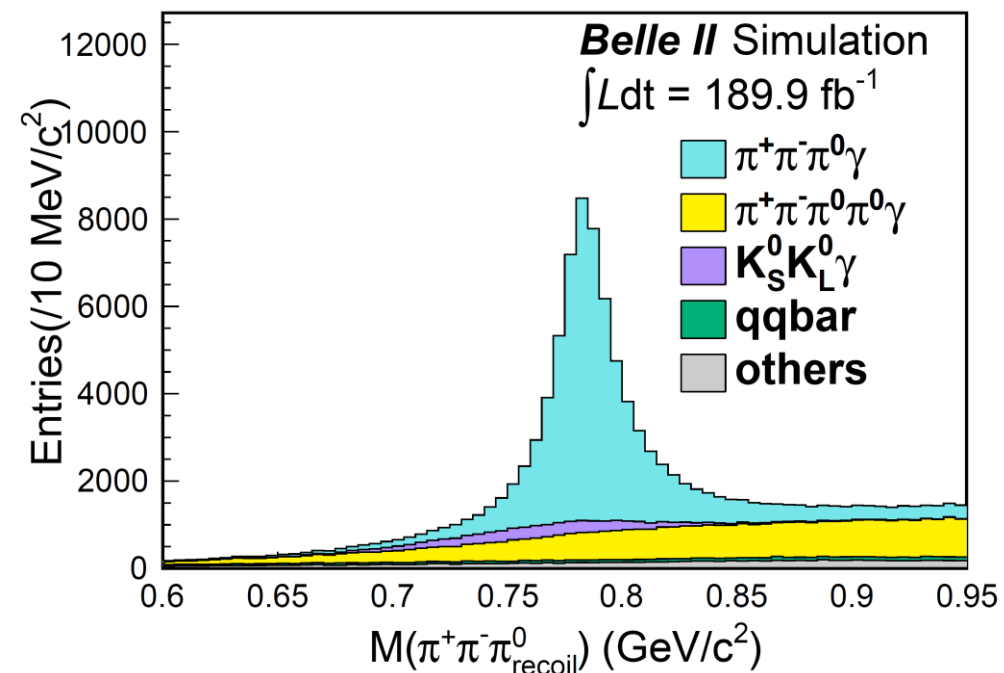
$$\pi^0 \text{ efficiency} = \frac{N(\text{Full reconstruction} : \gamma_{\text{ISR}}\pi^+\pi^-\pi^0)}{N(\text{Partial reconstruction} : \gamma_{\text{ISR}}\pi^+\pi^-)}$$

Partial reconstruction $\pi^+\pi^-\gamma$: ISR + Two tracks

- Kinematic fit to $\pi^+\pi^-\gamma$ with hypothesis that recoil mass equals π^0 mass. (1-constraint)
- Fit on $M(\pi^+\pi^-\pi^0_{\text{recoil}})$ distribution around ω resonance to estimate the number of $3\pi\gamma$.
 - Count the number of events in ω region.

$$M^2(\pi^+\pi^-\pi^0_{\text{recoil}}) = (p_{\pi^+} + p_{\pi^-} + p_{\text{recoil}})^2$$

$M(\pi^+\pi^-\pi^0_{\text{recoil}})$ distribution



π^0 efficiency correction

π^0 detection efficiency is 50-60%.

Evaluate efficiency using the $e^+e^- \rightarrow \pi^+\pi^-\pi^0\gamma$ events of ω resonance.

$$\pi^0 \text{ efficiency} = \frac{N(\text{Full reconstruction} : \gamma_{\text{ISR}}\pi^+\pi^-\pi^0)}{N(\text{Partial reconstruction} : \gamma_{\text{ISR}}\pi^+\pi^-)}$$

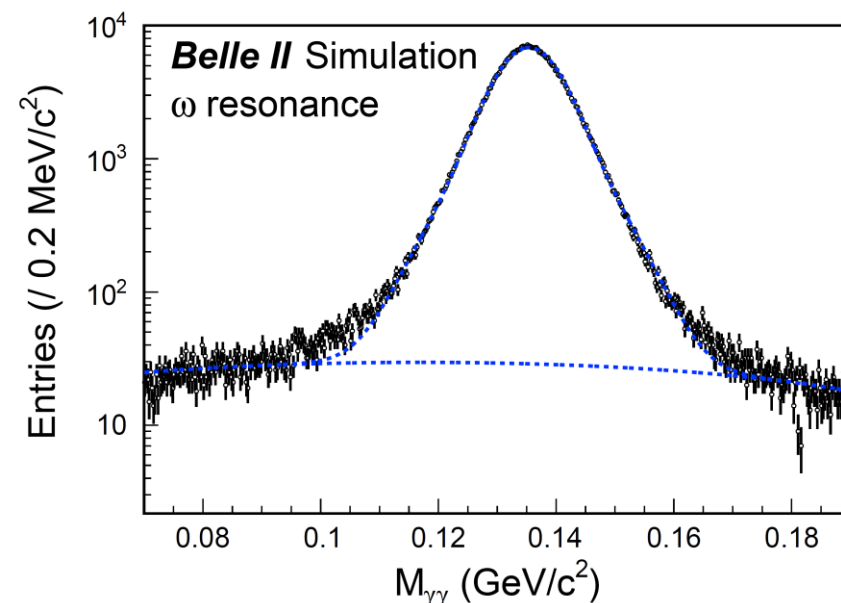
Full reconstruction : Partial reconstruction + π^0 selection + $\chi^2_{4C,3\pi\gamma} < 50$

- Fit $M(\gamma\gamma)$ with signal extraction parameters at ω region events
 - Signal : Novosibirsk function + Gaussian (Fixed parameters)
 - Background : Quadratic function (Floated parameters)

The systematic uncertainty related to π^0 is 1.0%.

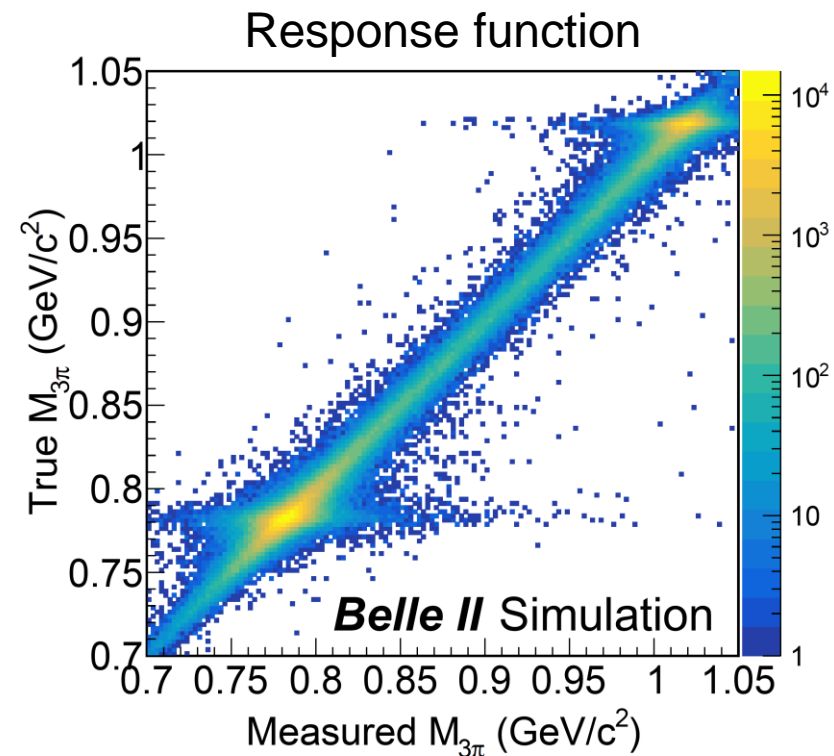
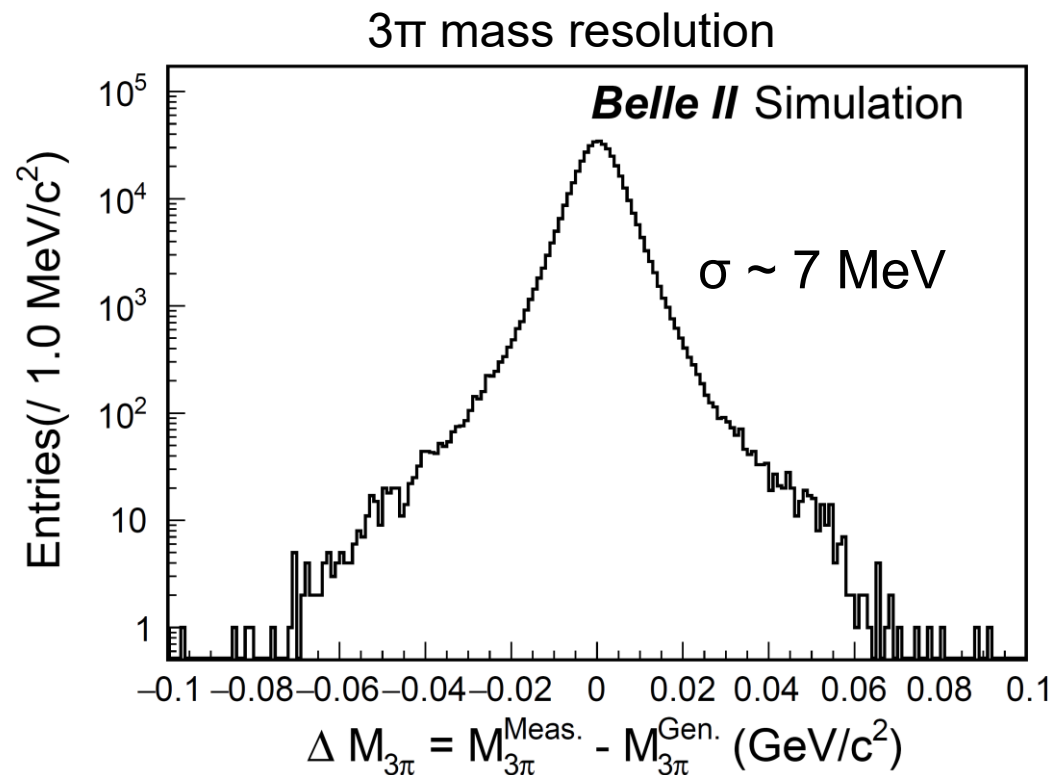
- The uncertainty is evaluated by variations of the $M(\gamma\gamma)$ signal pdf, background pdfs, and selections.

$M(\gamma\gamma)$ fit (Simulation)



Unfolding

- The background-subtracted spectrum is unfolded to mitigate the effect of detector response and final-state radiation.
- The data-MC resolution difference is determined by a Gaussian convolution fit to the ω , Φ , and J/ψ resonances.
 - The agreement is good typically with a mass resolution around 7-10 MeV.



Systematic uncertainty and prospects

- Major systematic uncertainty comes from π^0 and tracking.
 - In $M(3\pi) > 1.05$ GeV, the uncertainty of selection efficiency is dominant.
- For $a_\mu(3\pi)$, the total uncertainty is expected to be 2% including stat. uncertainty of 0.5%.
- The results will be released within a few months.

Systematic uncertainties for $e^+e^- \rightarrow \pi^+\pi^-\pi^0$ cross section (Preliminary)

Source	Systematic uncertainty (%)	
	$M < 1.05$ GeV c^2	$M > 1.05$ GeV c^2
Trigger	0.2	0.2
ISR photon detection	0.7	0.7
Tracking	0.8	0.8
π^0 reconstruction	1.0	1.0
χ^2 distribution	0.3	0.3
Selection	0.2	1.9
Integrated luminosity	0.7	0.7
Radiative correction	0.5	0.5
Total systematics	1.8	2.61

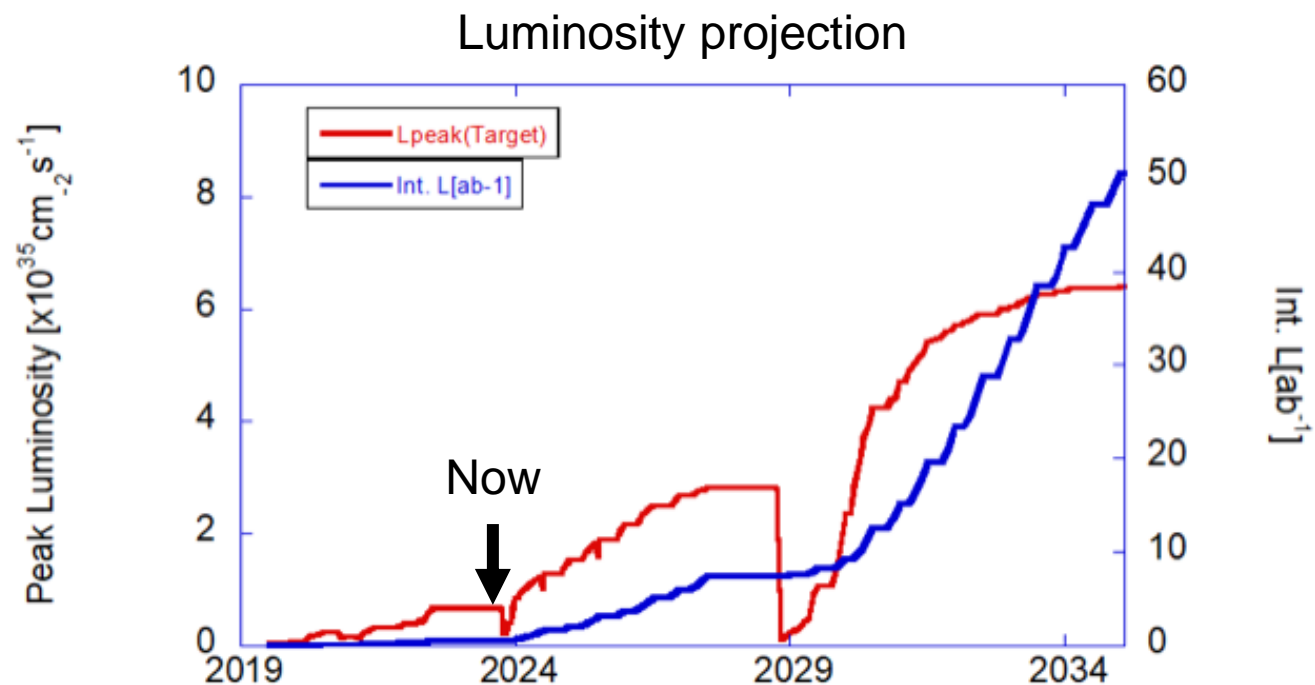
Conclusion

- Belle II has collected 424 fb⁻¹ data, and further data taking will be going on for over 10 years
 - Long shutdown 1 is finishing and new run will start from the end of 2023
- Measurements related to muon g-2 are active and in progress at Belle II
- The analysis of $e^+e^- \rightarrow \pi^+\pi^-$ targets 0.5% precision
- The analysis of $e^+e^- \rightarrow \pi^+\pi^-\pi^0$ is at the final stage
 - We aim at ~2% precision using 190 fb⁻¹ data
 - Blind analysis is introduced
 - Major systematic uncertainty comes from π^0 and tracking
 - The results will be released within a few months

Backup

Operation Plans

- Long Shutdown 1 is finishing and new run will start end of 2023.
 - SuperKEKB upgrade for higher luminosity etc.
 - Full coverage of pixel detector
 - PMT replacement of the barrel PID detector for lifetime and robustness
 - Data-acquisition system upgrade
- Another long shutdown around 2027 is under discussion.



$e^+e^- \rightarrow \pi^+\pi^-$: Status at Belle II

- Target precision : 0.5% of $a_\mu(2\pi)$
- Trying to follow BaBar methods as a base line.
- Systematics uncertainty dominant analysis
 - BaBar : 232 /fb [Phys. Rev. D 86 (2012), 032013]
 - We can use large statistics to control systematic uncertainties.
- Implementation of kinematic fitting tools
 - Useful for reducing background and correction for tracking efficiency.
 - Implementation of basic fitter has been completed.

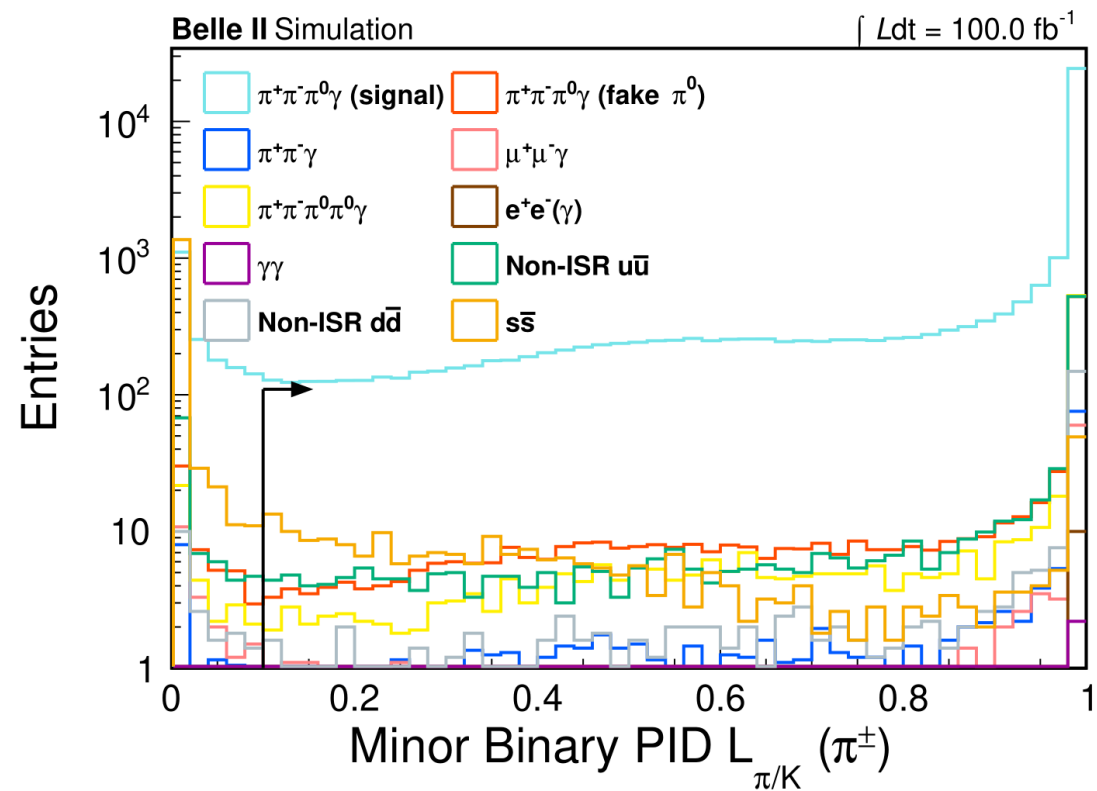
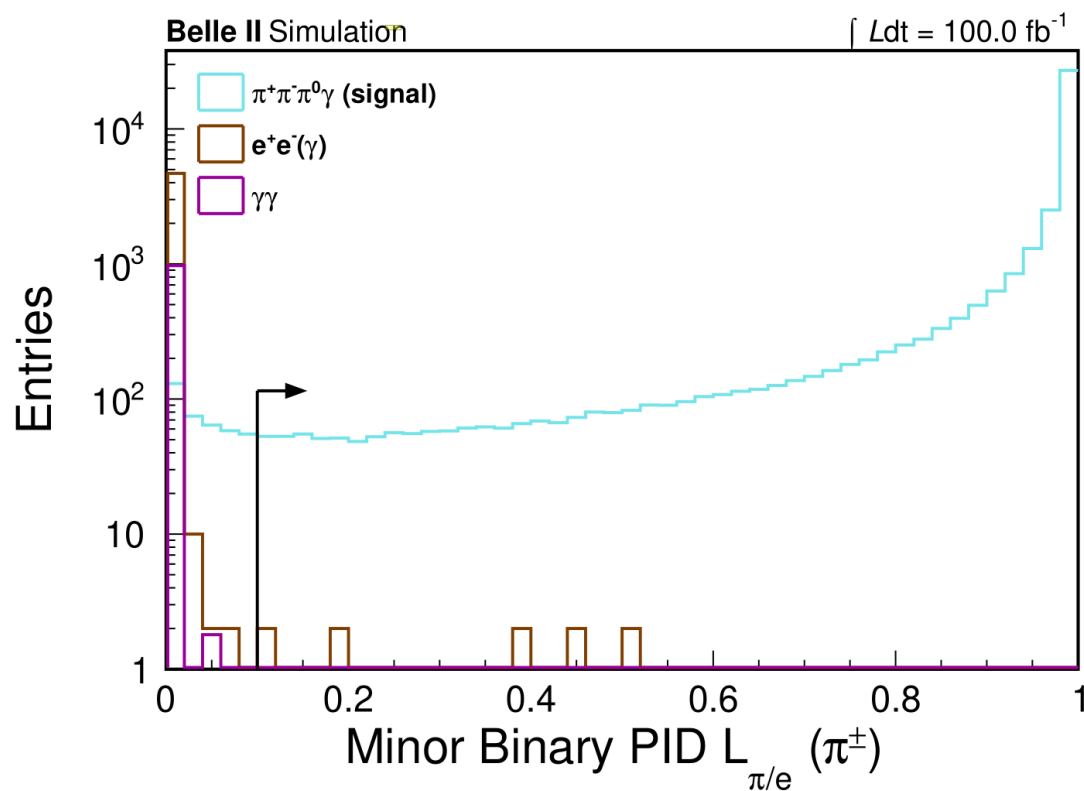
- Sanity check on signal generator and background MC using $< 2 \text{ fb}^{-1}$ data .
- Design of data-driven efficiency corrections for tracking, trigger and $\pi/\mu/K$ ID is ongoing.

$ee \rightarrow \pi\pi$ uncertainty (10^{-3}) at BaBar

Sources	0.3–0.4	0.4–0.5	0.5–0.6	0.6–0.9	0.9–1.2
Trigger/filter	5.3	2.7	1.9	1.0	0.7
Tracking	3.8	2.1	2.1	1.1	1.7
π -ID	10.1	2.5	6.2	2.4	4.2
Background	3.5	4.3	5.2	1.0	3.0
Acceptance	1.6	1.6	1.0	1.0	1.6
Kinematic fit (χ^2)	0.9	0.9	0.3	0.3	0.9
Correl. $\mu\mu$ ID loss	3.0	2.0	3.0	1.3	2.0
$\pi\pi/\mu\mu$ non-cancel.	2.7	1.4	1.6	1.1	1.3
Unfolding	1.0	2.7	2.7	1.0	1.3
ISR luminosity	3.4	3.4	3.4	3.4	3.4
Sum (cross section)	13.8	8.1	10.2	5.0	6.5

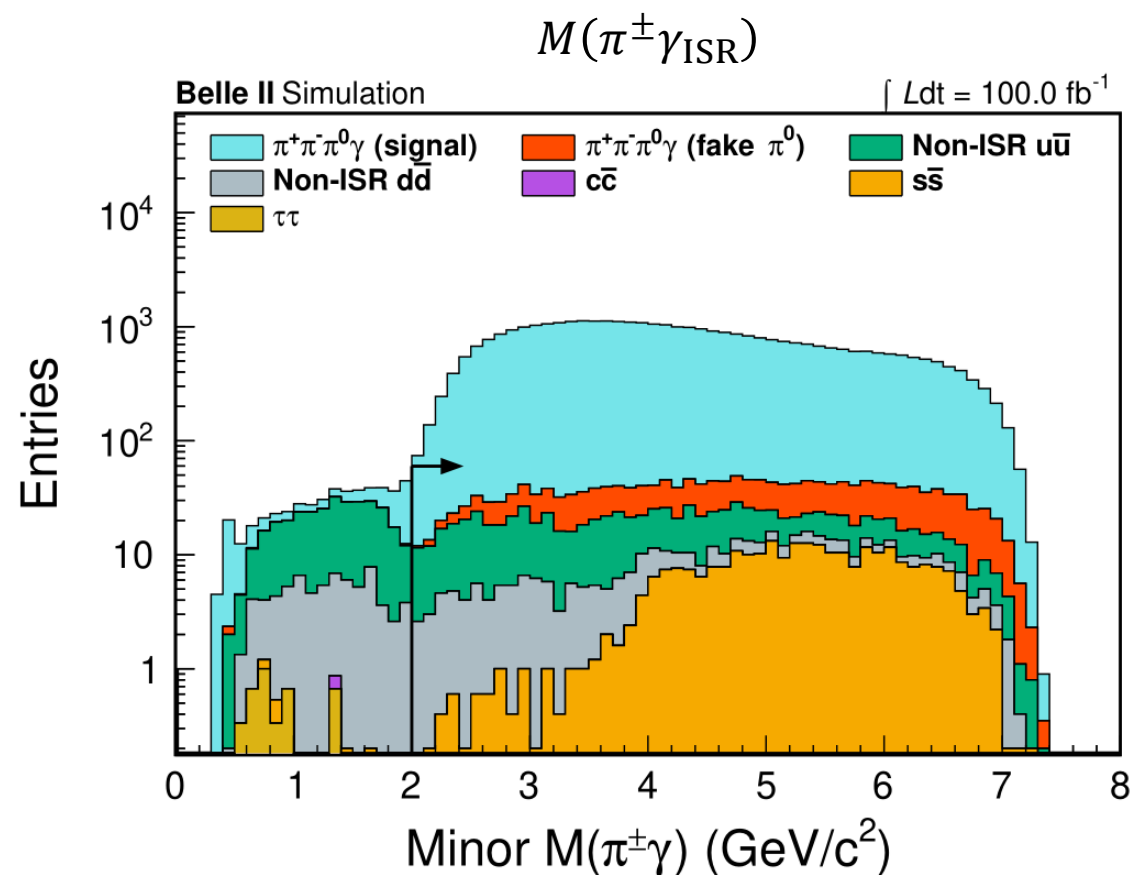
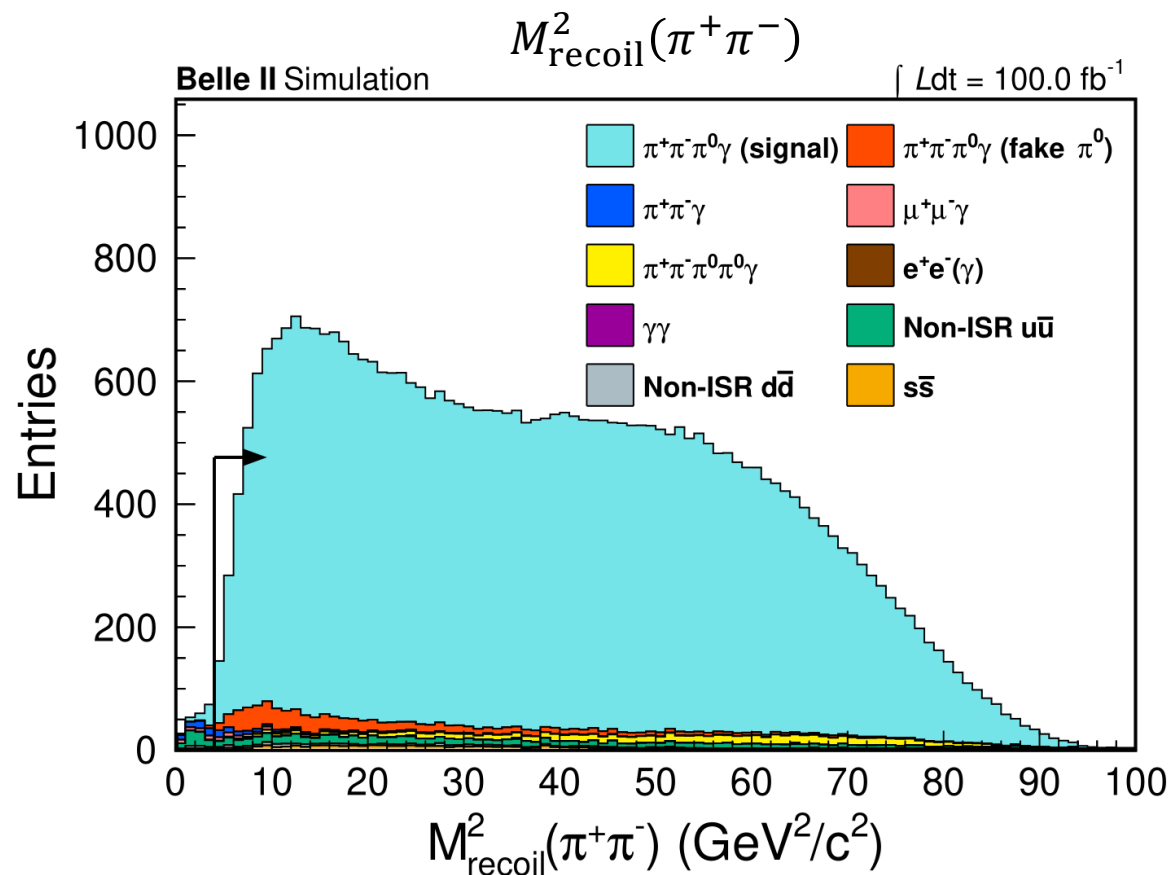
Event selection : Background reduction cuts

- Electron- and kaon-related backgrounds
 - $L(\pi/e) > 0.1$ for both tracks (no SVD and noTOP)
 - $L(\pi/K) > 0.1$ for both tracks



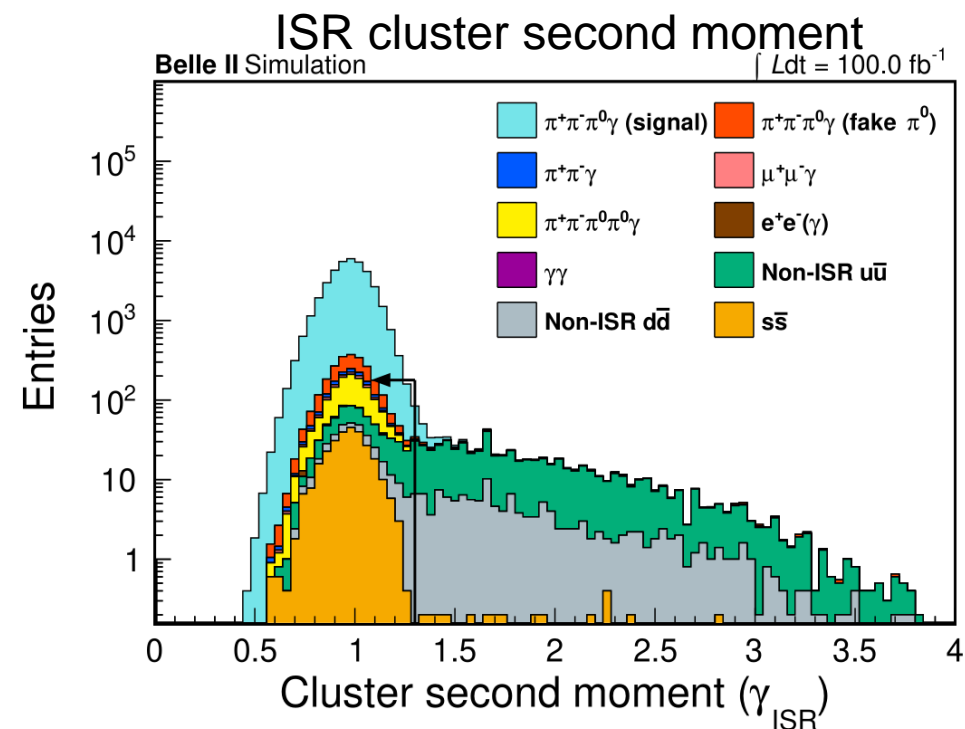
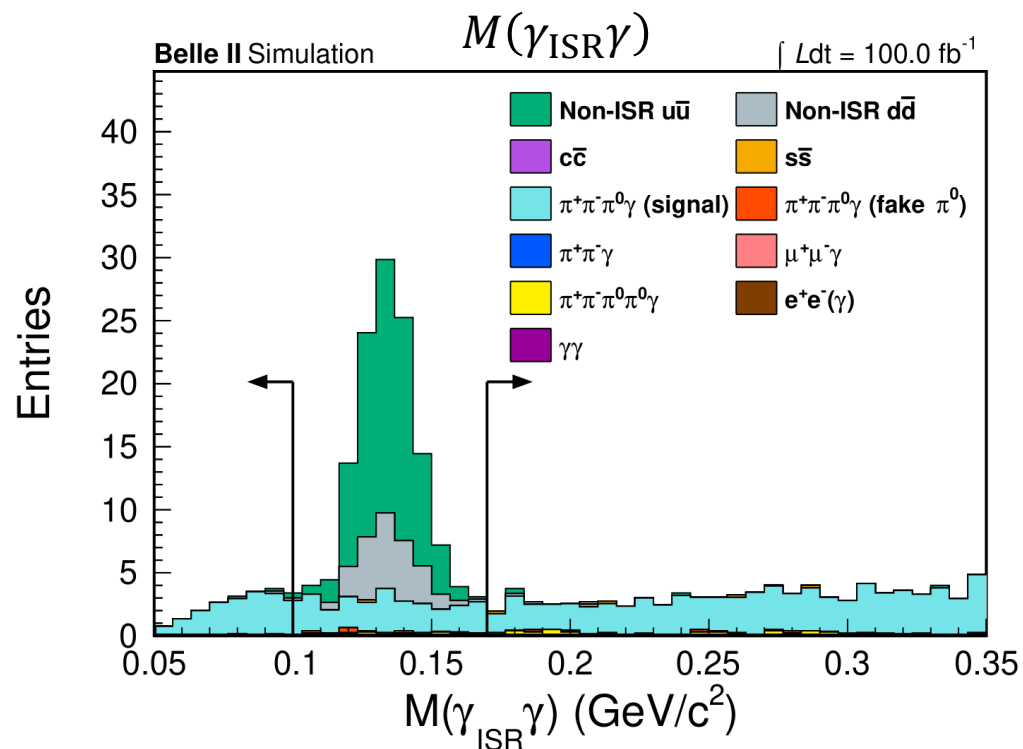
Event selection : Background reduction cuts

- $M_{\text{recoil}}^2(\pi^+\pi^-) > 4 \text{ GeV}^2$ for $\pi^+\pi^-\gamma$ and $\mu^+\mu^-\gamma$ rejection
- Non-ISR qqbar and $\tau\tau$ reduction (1)
 - $M(\pi^\pm\gamma_{\text{ISR}}) > 2 \text{ GeV}$ to reduce $\rho^\pm \rightarrow \pi^+\pi^0(\rightarrow \gamma\gamma)$



Event selection : Background reduction cuts

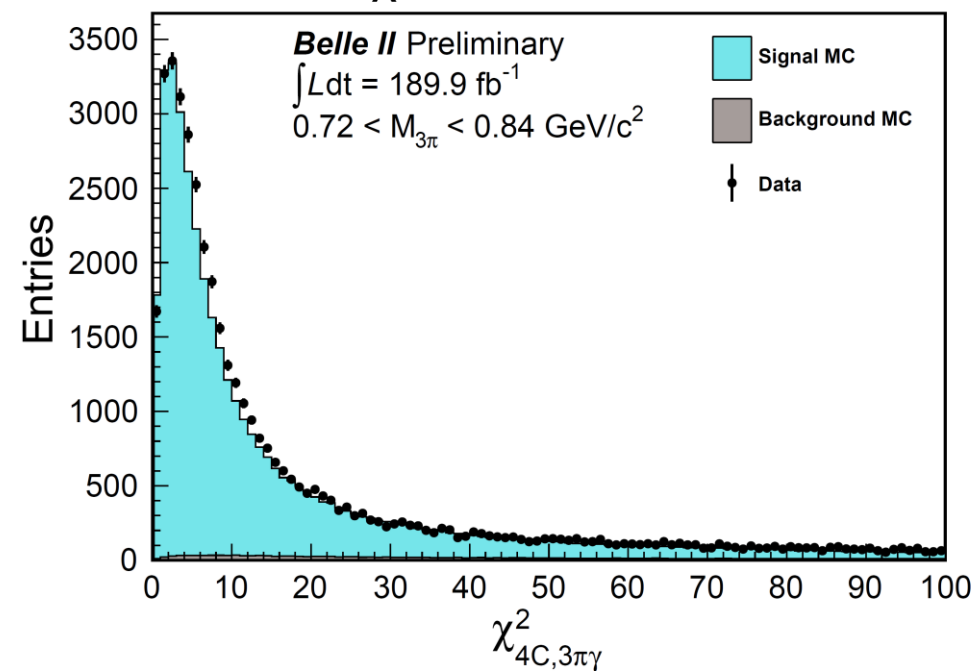
- Non-ISR qqbar and τ reduction (2)
 - One daughter photon of π^0 is reconstructed as ISR
 - Reconstruct π^0 from ISR and additional photon
 - Reject the invariant mass $0.110 < M(\gamma_{\text{ISR}}\gamma) < 0.170$ GeV
 - Both photon clusters of π^0 decay are merged and reconstructed as ISR
 - Cluster second moment of ISR < 1.3



$e^+e^- \rightarrow \pi^+\pi^-\pi^0$: Event selection

- Two tracks + three photons : $e^+e^- \rightarrow \pi^+\pi^-\pi^0\gamma_{ISR} \rightarrow \pi^+\pi^-\gamma\gamma\gamma_{ISR}$
 - Tracks : originate from the interaction point + $p_T > 0.2$ GeV
 - Photons : $E > 100$ MeV + at least one photon must be energetic ISR ($E^{CMS} > 2$ GeV in barrel ECL)
- π^0 reconstruction
 - Invariant mass of two photons within 0.123-0.147 GeV/ c^2
- Select events using four-momentum kinematic fit (4C-Kfit) χ^2
 - $\chi^2_{4C}(3\pi\gamma) < 50$ is used for the cross section measurement.
- Reduce backgrounds by additional cuts (next pages)

4C-Kfit χ^2 at the ω resonance



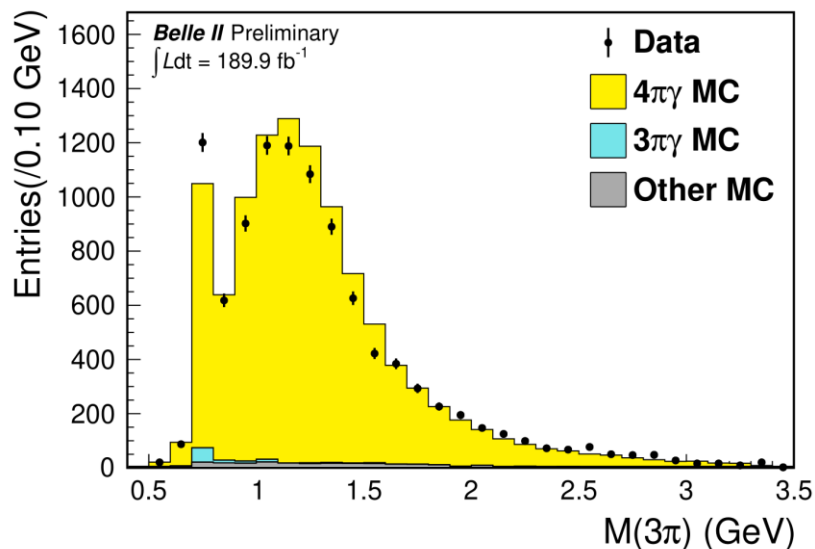
$e^+e^- \rightarrow \pi^+\pi^-\pi^0$: Background estimation

Estimate by determining a mass-dependent data-MC scale factor using a control sample (CS)

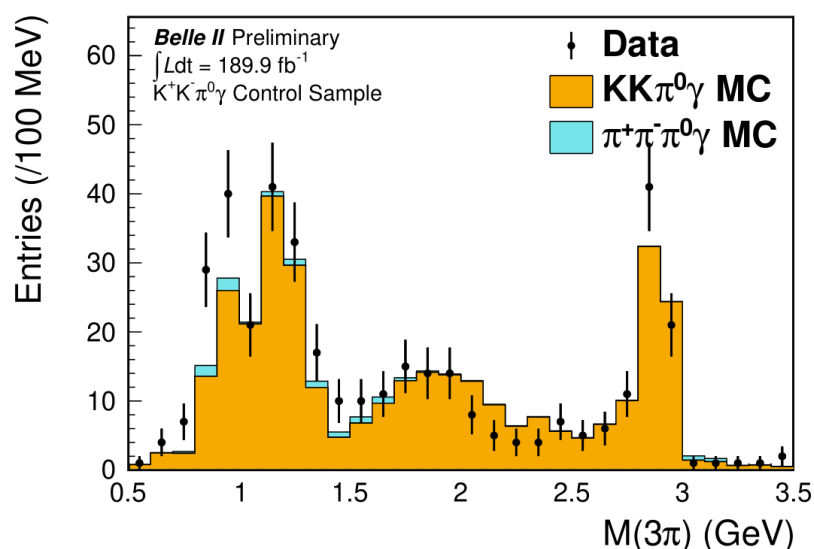
$$N_{SS}^{\text{data}} = N_{SS}^{\text{MC}} \cdot \frac{N_{CS}^{\text{data}}}{N_{CS}^{\text{MC}}}$$

- $\pi^+\pi^-\pi^0\pi^0\gamma$: Reconstruct $\pi^+\pi^-\pi^0\pi^0\gamma$ and select $\chi^2(4\pi\gamma) < 30$
- $K^+K^-\pi^0\gamma$: Invert binary π/K ID : $L(\pi/K) > 0.1 \Rightarrow L(\pi/K) < 0.1$
- Non-ISR $q\bar{q}$ (dominated by $\pi^+\pi^-\pi^0\pi^0$) : $0.10 < M(\gamma_{\text{ISR}}\gamma) < 0.17$ GeV / large cluster second moment

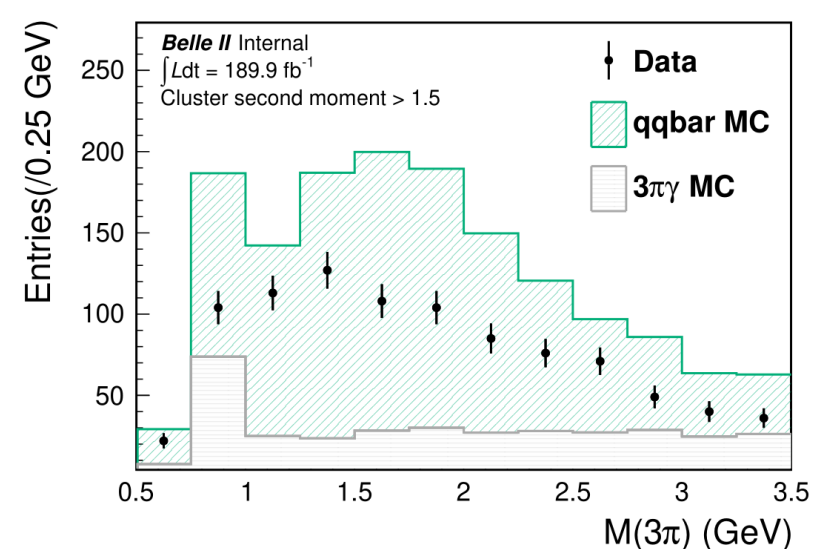
4 $\pi\gamma$ control sample



KK $\pi^0\gamma$ control sample

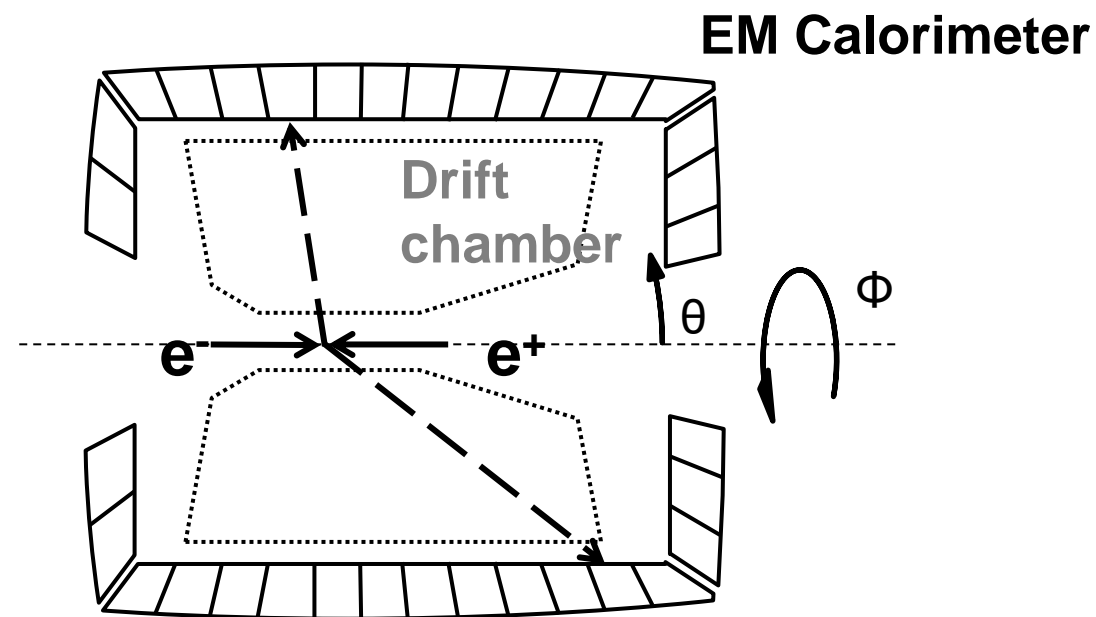


Non-ISR $q\bar{q}$ control sample



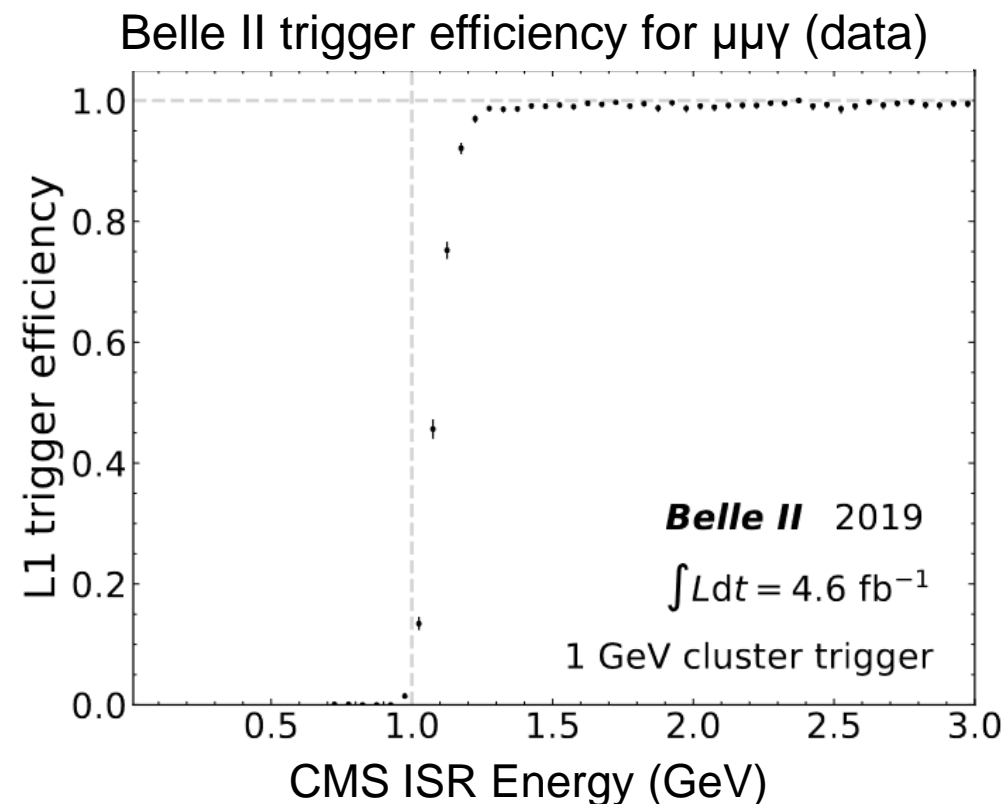
Trigger challenge at Belle II

- Light hadron cross section measurement at BELLE was suffered from the trigger efficiency.
 - The measurement for $\sigma(e^+e^- \rightarrow \pi^+\pi^-\pi^0)$ was attempted, but could not be published.
[J. Crnkovic, PhD thesis, Illinois U. (2013)]
- Bhabha veto has been upgraded to avoid the inefficiency and uncertainty.
 - BELLE bhabha veto was based on only θ angle.
 - Belle II 3D bhabha veto uses θ and Φ angle.
- The trigger efficiency of EM Calorimeter triggers for energetic ISR can be measured by making the orthogonal tracking trigger a reference.



Trigger challenge at Belle II

- Light hadron cross section measurement at BELLE was suffered from the trigger efficiency.
 - The measurement for $\sigma(e^+e^- \rightarrow \pi^+\pi^-\pi^0)$ was attempted, but could not be published.
[J. Crnkovic, PhD thesis, Illinois U. (2013)]
- Bhabha veto has been upgraded to avoid the inefficiency and uncertainty.
 - BELLE bhabha veto was based on only θ angle.
 - Belle II 3D bhabha veto uses θ and Φ angle.
- The trigger efficiency of EM Calorimeter triggers for energetic ISR can be measured by making the orthogonal tracking trigger a reference.
 - Efficiency for energetic ISR > 99%
 - Event loss due to 3D bhabha veto is suppressed in $\mu\mu\gamma$.
- The high trigger efficiency for energetic ISR is beneficial for most light hadron cross section measurements in the radiative return method.

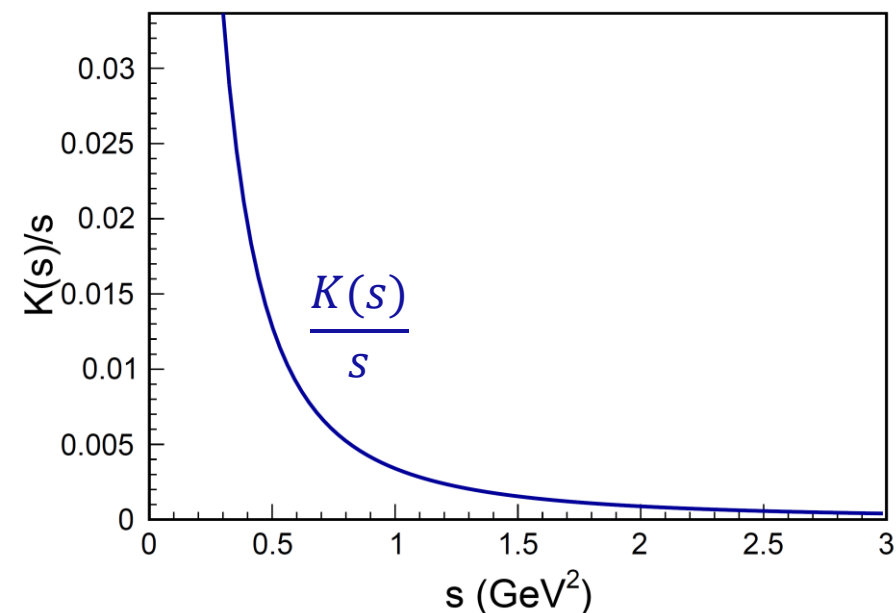


Data-driven method and R-ratio measurement

Leading order HVP contribution using dispersion relation

$$a_{\mu}^{\text{HVP,LO}} = \frac{\alpha^2}{3\pi^2} \int_{m_{\pi}^2}^{\infty} \frac{K(s)}{s} R(s) ds$$

$$R(s) = \frac{\sigma(e^+e^- \rightarrow \text{hadrons})}{\sigma(e^+e^- \rightarrow \mu^+\mu^-)}$$



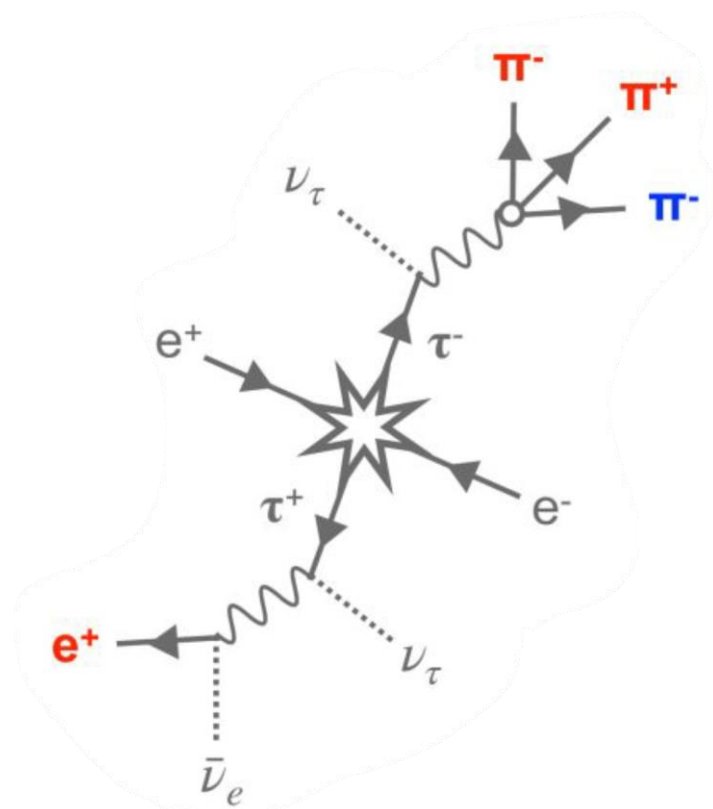
Kernel function

$$K(s) = \frac{x^2}{2} (2 - x) + \frac{(1 + x^2)(1 + x)^2}{x^2} \left(\ln(1 + x) - x + \frac{x^2}{2} \right) + \frac{1 + x}{1 - x} x^2 \ln(x)$$

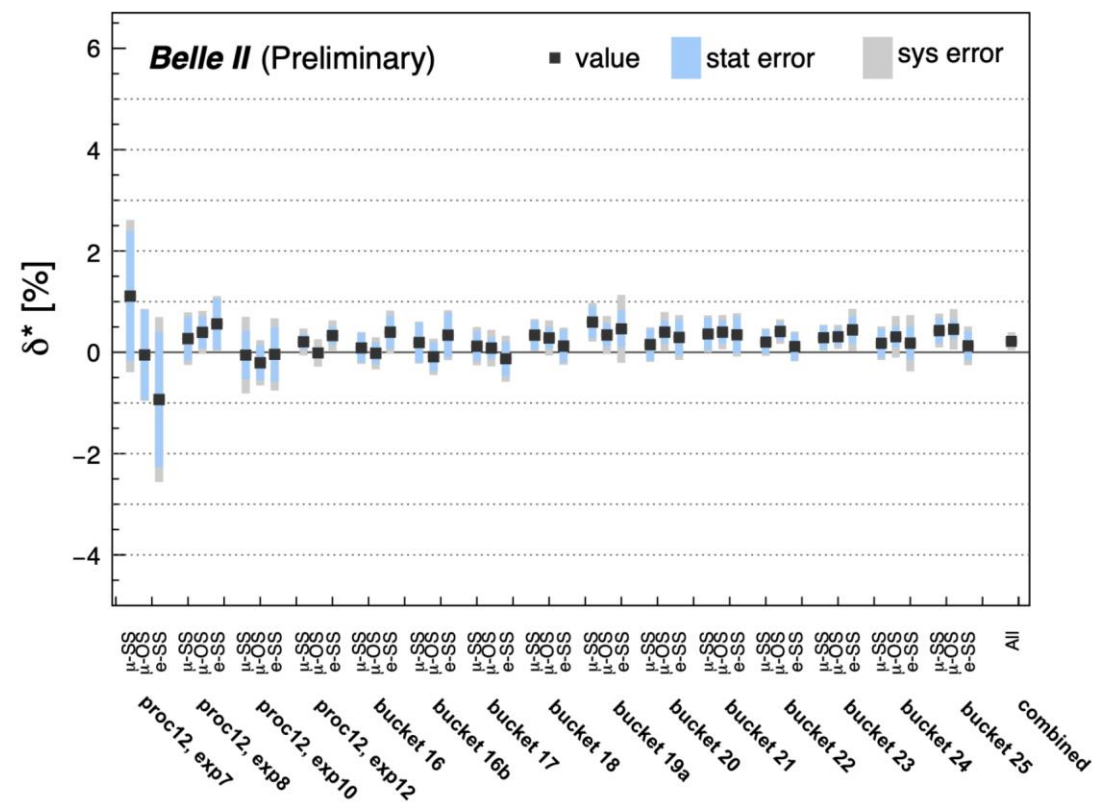
$$x = \frac{1 - \beta_{\mu}}{1 + \beta_{\mu}}, \quad \beta_{\mu} = \sqrt{1 - \frac{4m_{\mu}^2}{s}}$$

Performance : Tracking Efficiency

- Tracking efficiency is measured by tag-and-probe method on $ee \rightarrow \tau\tau \rightarrow 1 \times 3$ prong.
 - 3 good quality tracks for **tag**
 - Look for 4th track for **probe**
- Uncertainty for tracking efficiency is 0.30% per track.

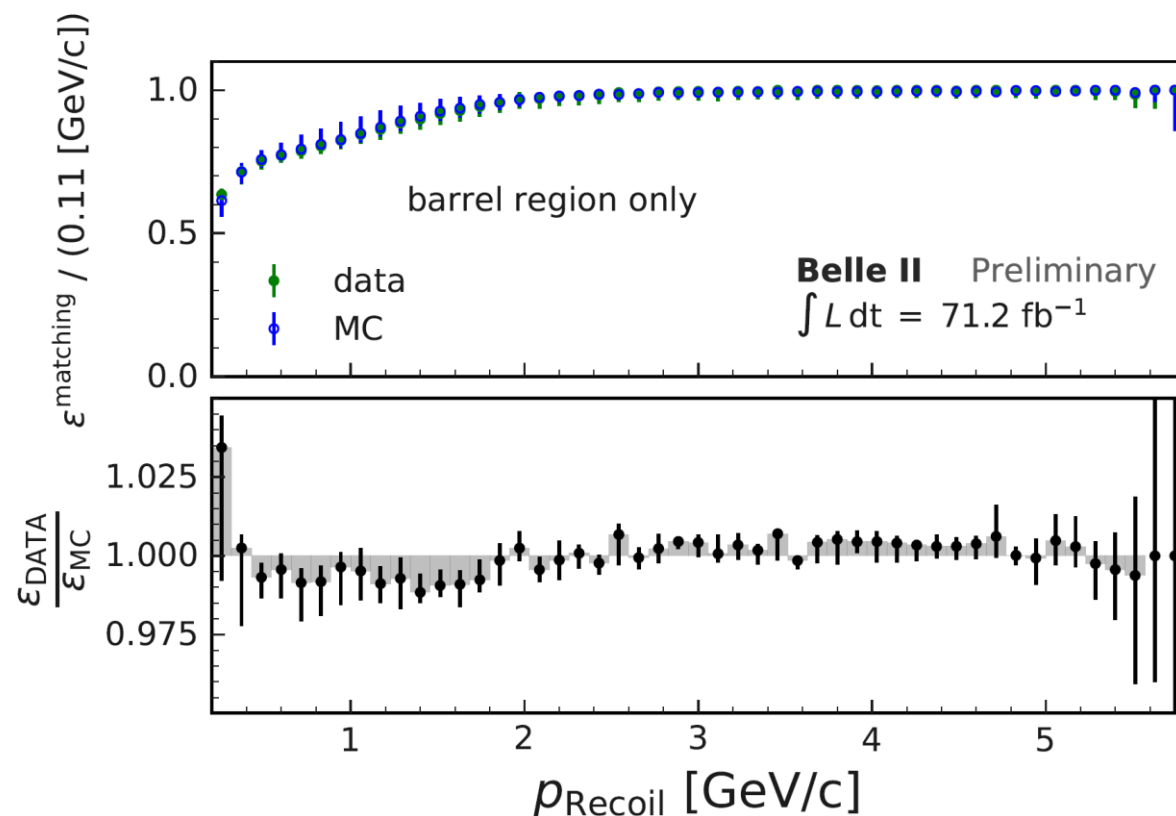
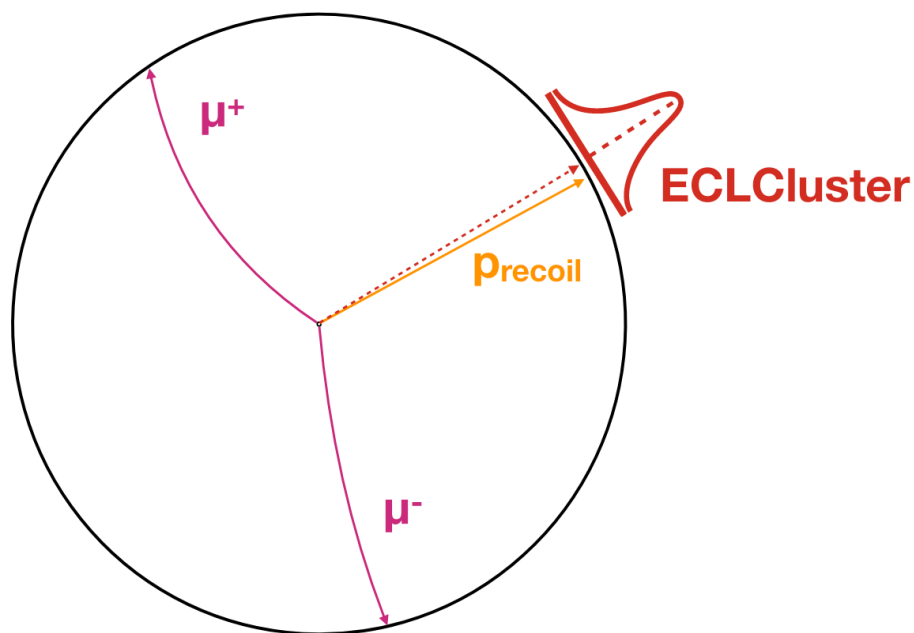


Data/MC discrepancy of tracking efficiency



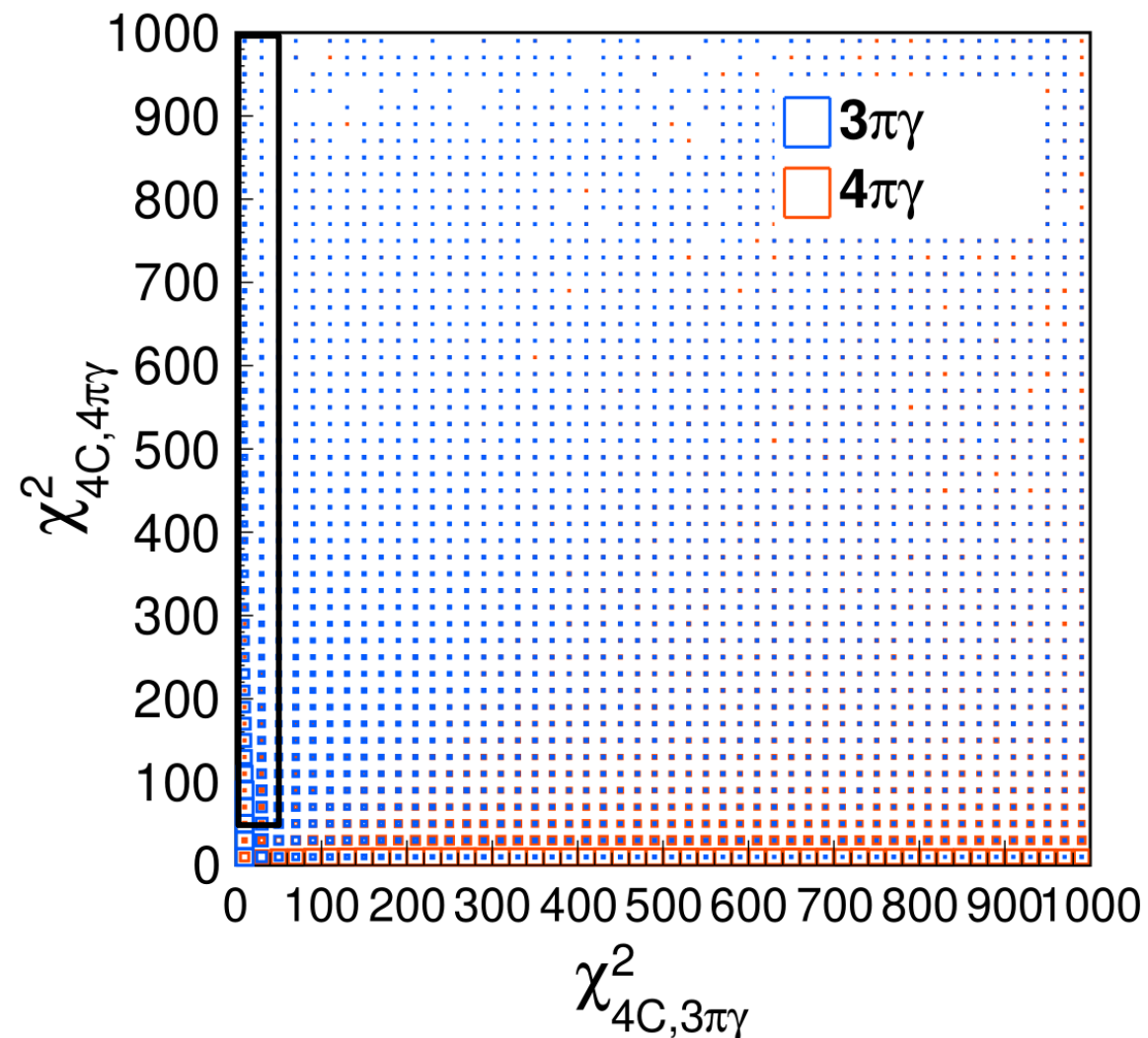
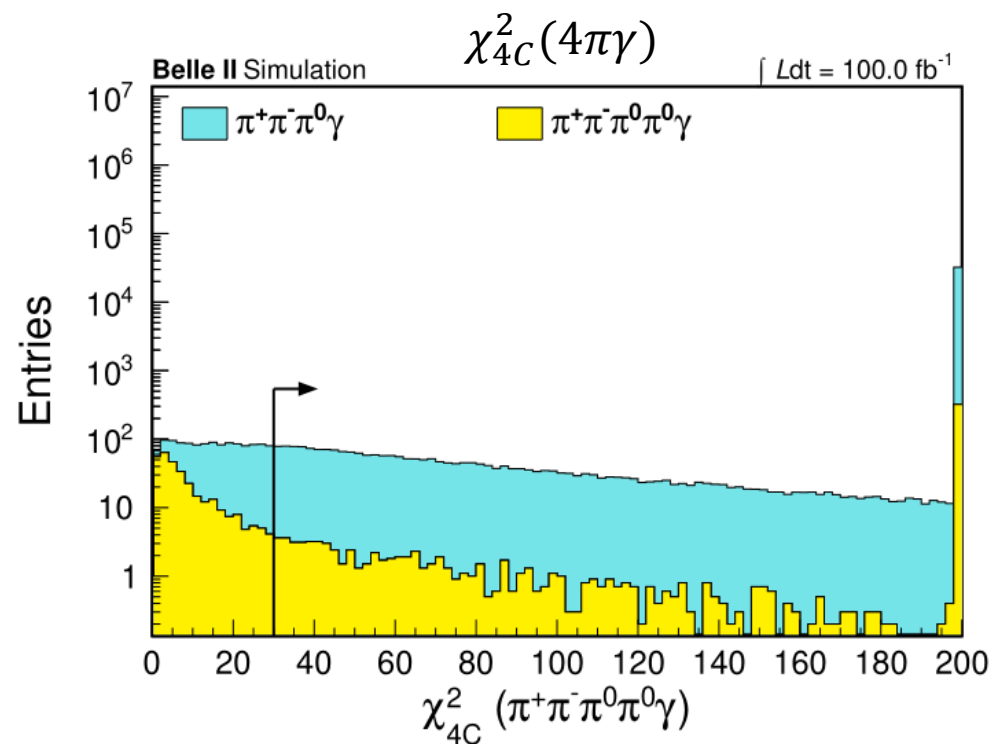
Performance : Photon Detection Efficiency

- Photon detection efficiency is measured using $ee \rightarrow \mu\mu\gamma$ events.
 - Detection efficiency is estimated by taking match between a ECL cluster and the missing momentum of dimuon system.
- Data/MC agreement is good. Uncertainty for photon detection efficiency is 0.30%.

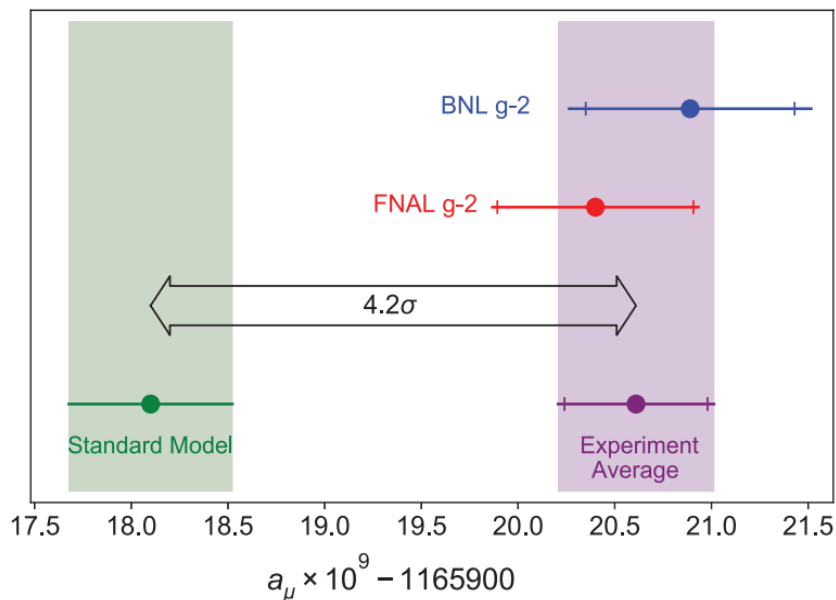


Event selection : Background reduction cuts

- $\pi^+\pi^-\pi^0\pi^0\gamma$ rejection
 - Reconstruct $\pi^+\pi^-\pi^0\pi^0\gamma$ from additional π^0
 - Apply 4C-Kfit under $\pi^+\pi^-\pi^0\pi^0\gamma$ hypothesis
 - $\chi_{4C,4\pi\gamma}^2 > 30$

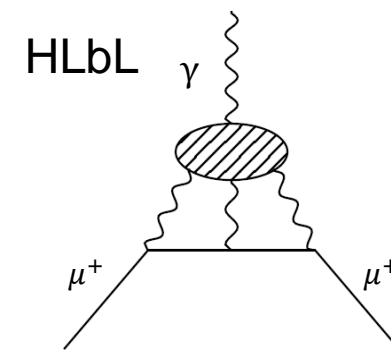
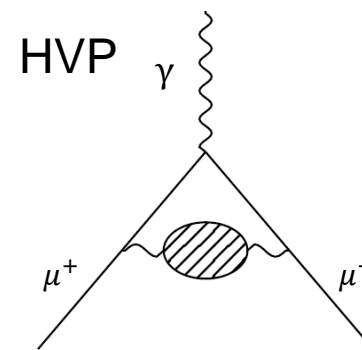
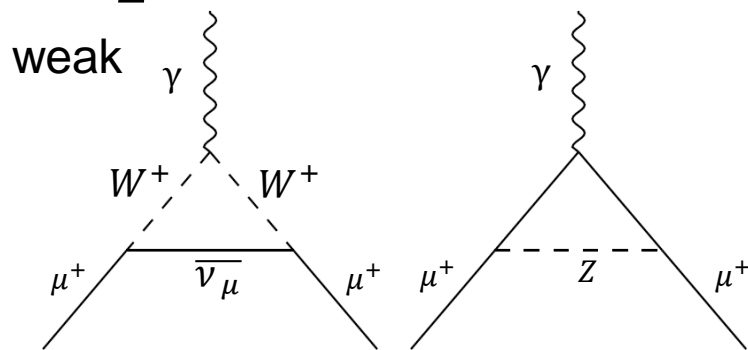
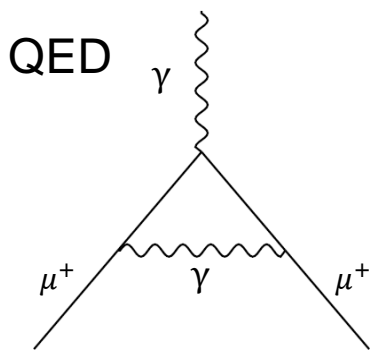


Introduction for muon $g-2$



Contribution	Value $a_\mu \times 10^{11}$	Error $\delta a_\mu \times 10^{11}$
QED	116 584 718.931	0.104
HVP LO (Leading-Order)	6931	40
HVP HO (Higher-Order)	-85.9	1.2
HLbL (Light-by-Light)	92	19
EW (Electroweak)	153.6	1
SM total (Dispersive)	116591810	43
Experiment (BNL+FNAL)	116592061	41
Experiment – SM	251	59

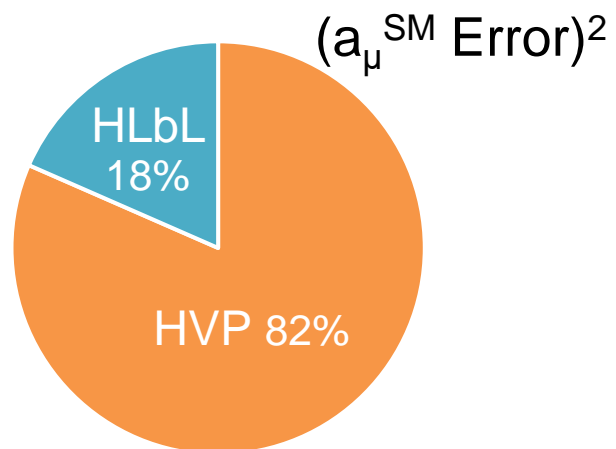
$$a_\mu^{\text{SM}} = \frac{g-2}{2} = a_\mu^{\text{QED}} + a_\mu^{\text{weak}} + a_\mu^{\text{HVP}} + a_\mu^{\text{HLbL}}$$



B. Abi *et al.*, PRL126, 141801 (2021)

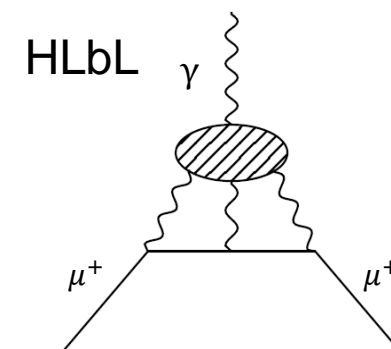
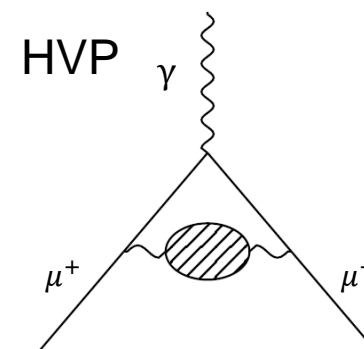
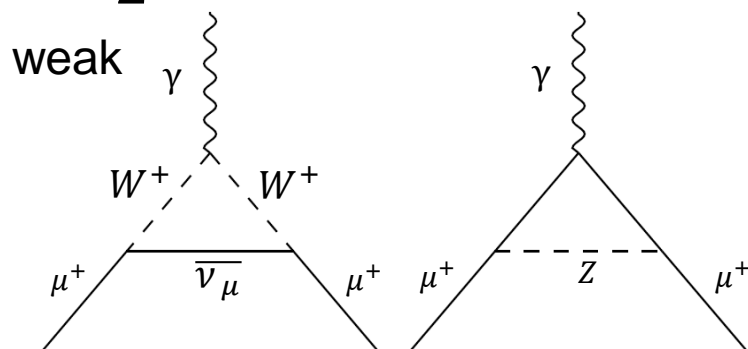
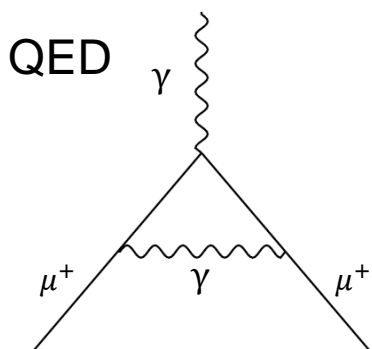
T. Aoyama *et al.*, Phys. Rept. 887 (2020).

Introduction for muon $g-2$



Contribution	Value $a_\mu \times 10^{11}$	Error $\delta a_\mu \times 10^{11}$
QED	116 584 718.931	0.104
HVP LO (Leading-Order)	6931	40
HVP HO (Higher-Order)	-85.9	1.2
HLbL (Light-by-Light)	92	19
EW (Electroweak)	153.6	1
SM total (Dispersive)	116591810	43
Experiment (BNL+FNAL)	116592061	41
Experiment – SM	251	59

$$a_\mu^{\text{SM}} = \frac{g-2}{2} = a_\mu^{\text{QED}} + a_\mu^{\text{weak}} + a_\mu^{\text{HVP}} + a_\mu^{\text{HLbL}}$$

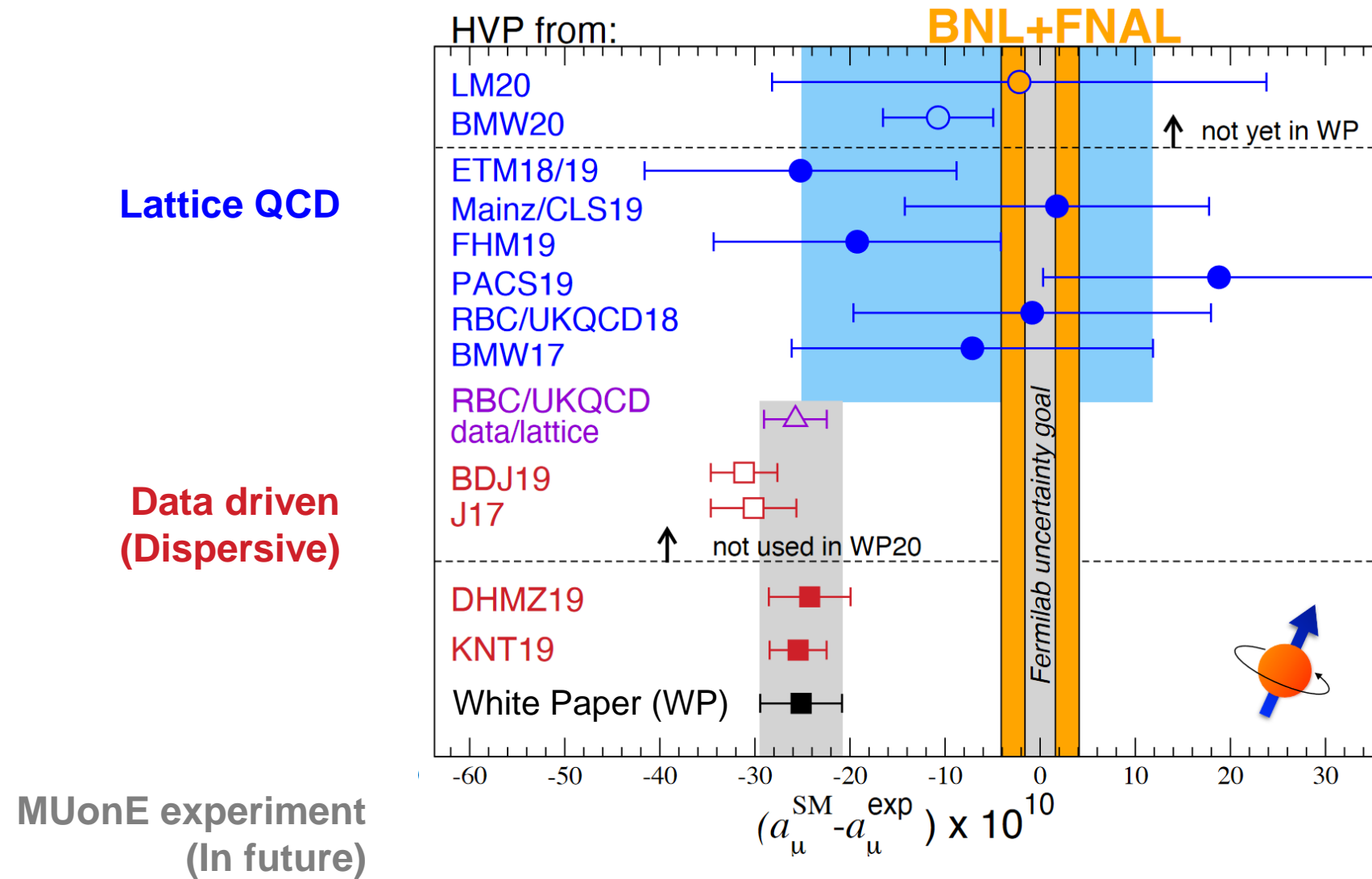


B. Abi *et al.*, PRL126, 141801 (2021)

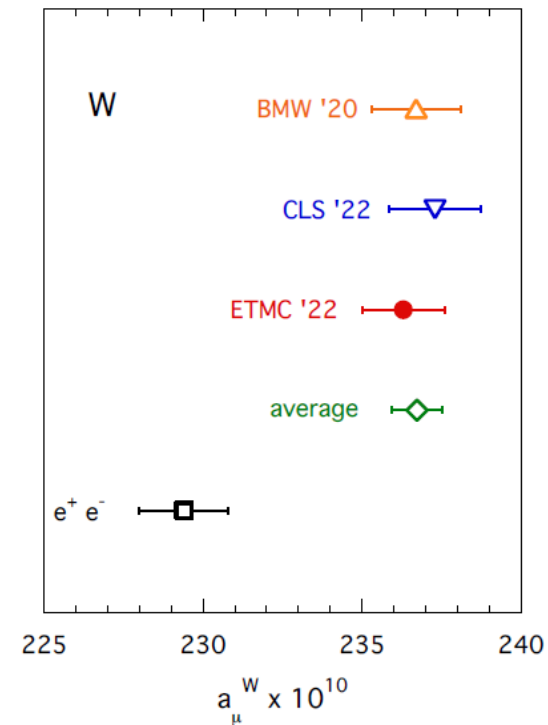
T. Aoyama *et al.*, Phys. Rept. 887 (2020).

HVP contribution

G. Colangelo *et al.*, arXiv:2203.15810 [hep-ex] (2022)

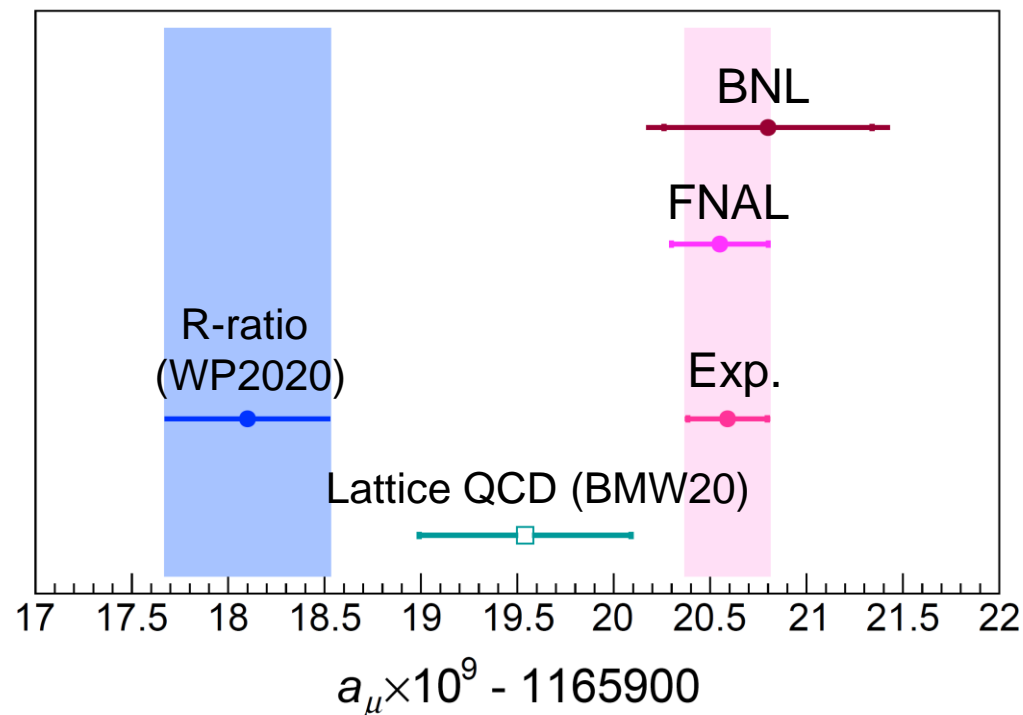


C. Alexandrou *et al.*, arXiv:2206.15084 [hep-lat] (2022)

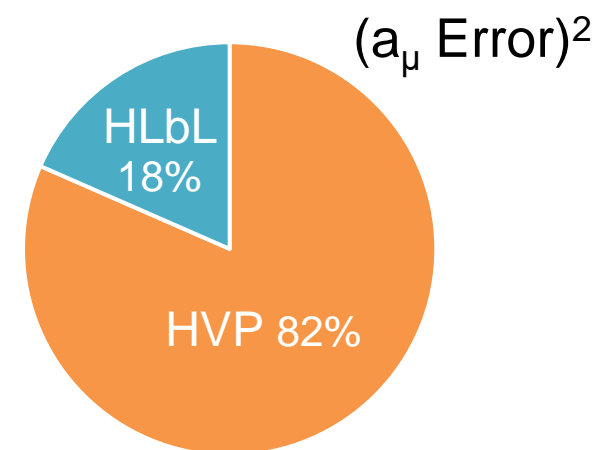


Muon $g-2$ and Hadronic Vacuum Polarization (HVP)

- HVP contributes to the largest uncertainty in the prediction of muon $g-2$.
- Two approaches for estimating the HVP contribution of SM predictions
 - Dispersion relations (w/ inputs from $ee \rightarrow$ hadrons data)
 - Lattice QCD
- Belle II can provide the cross section for $e^+e^- \rightarrow$ hadrons to improve the theoretical prediction.



$$a_\mu^{\text{SM}} = \frac{g-2}{2} = a_\mu^{\text{QED}} + a_\mu^{\text{EW}} + a_\mu^{\text{Had}}$$

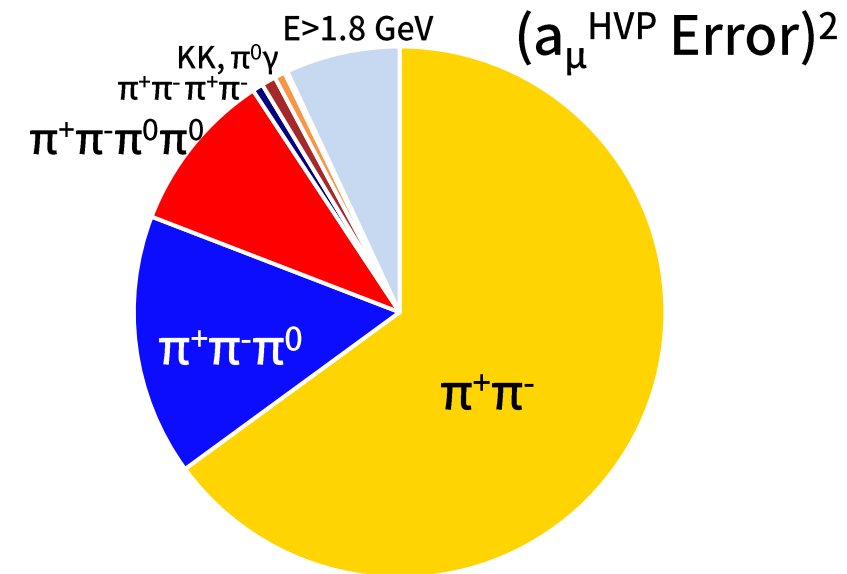
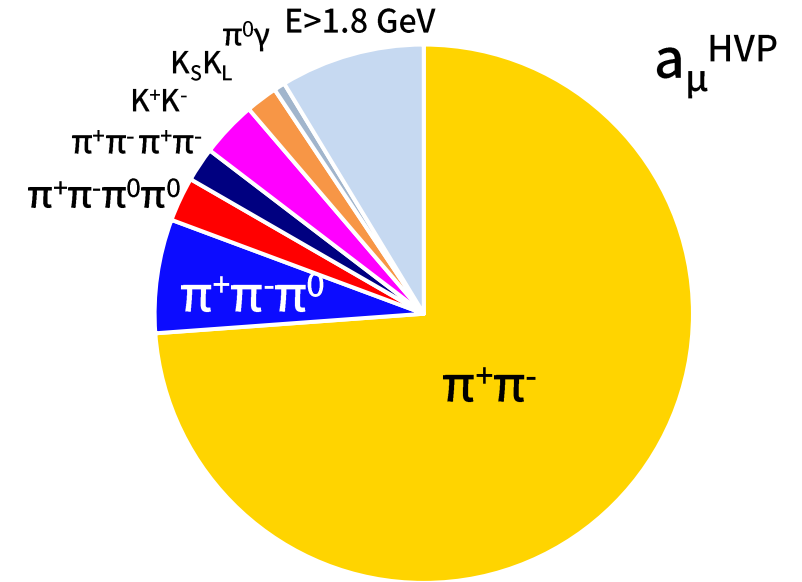
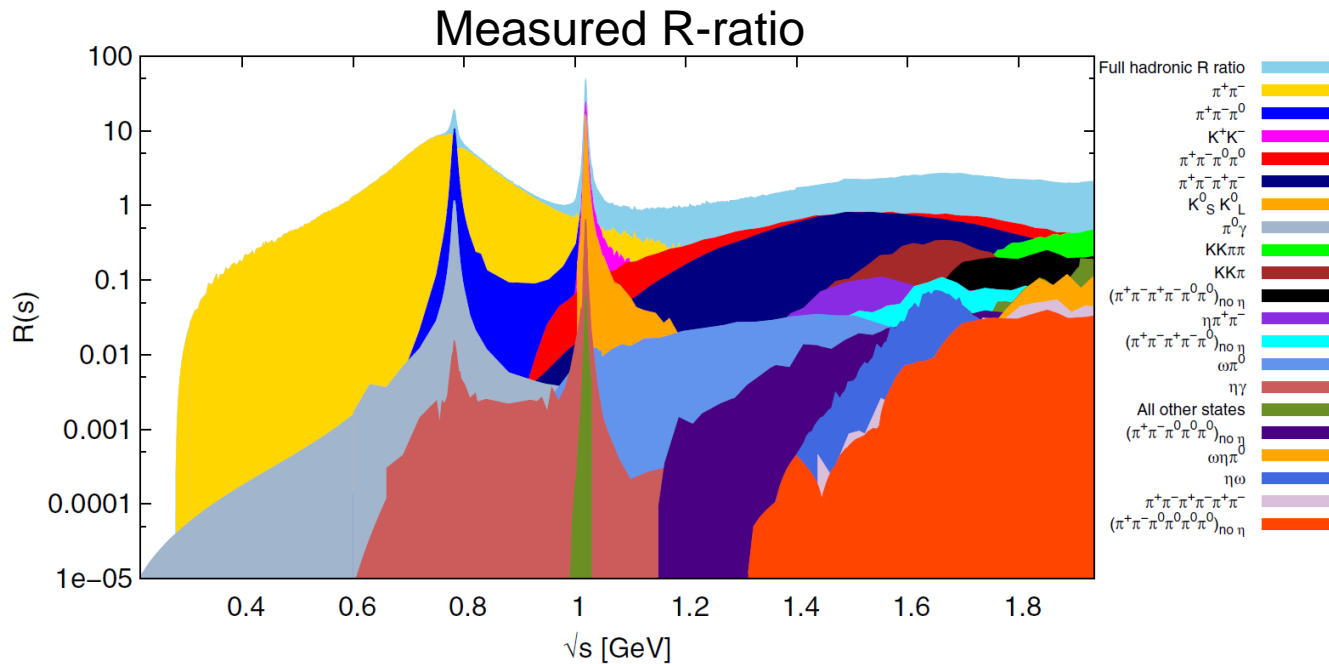


HVP measurement

Leading order HVP contribution using dispersion relation :

$$a_{\mu}^{\text{HVP,LO}} = \frac{\alpha^2}{3\pi^2} \int_{m_{\pi}^2}^{\infty} \frac{K(s)}{s} R(s) ds$$

$$R(s) = \frac{\sigma(e^+e^- \rightarrow \text{hadrons})}{\sigma(e^+e^- \rightarrow \mu^+\mu^-)} \quad K(s) : \text{QED kernel function}$$



R-ratio measurement

Leading order HVP contribution using dispersion relation :

$$a_{\mu}^{\text{HVP,LO}} = \frac{\alpha^2}{3\pi^2} \int_{m_{\pi}^2}^{\infty} \frac{K(s)}{s} R(s) ds$$

$$R(s) = \frac{\sigma(e^+e^- \rightarrow \text{hadrons})}{\sigma(e^+e^- \rightarrow \mu^+\mu^-)} \quad K(s) : \text{QED kernel function}$$

